

Review

# Supramolecular Association via Hg $\cdots$ S Secondary-Bonding Interactions in Crystals of Organomercury(II) Species: A Survey of the Cambridge Structure Database

Edward R. T. Tiekink 

Research Centre for Crystalline Materials, School of Medical and Life Sciences, Sunway University, Badar Sunway 47500, Selangor Darul Ehsan, Malaysia; edwardt@sunway.edu.my; Tel.: +60-374917181

**Abstract:** The Cambridge Structural Database has been surveyed for crystals featuring organo-Hg $\cdots$ S secondary-bonding interactions within supramolecular aggregates. Nearly 50% of crystals where Hg $\cdots$ S interactions could potentially form, featured Hg $\cdots$ S contacts within zero- or one-dimensional supramolecular assemblies with only a few examples of two-dimensional arrays featuring Hg $\cdots$ S interactions. This high propensity of Hg $\cdots$ S contact formation reflects the inherent thiophilic nature of mercury but also the relatively open access to mercury owing to the linear C–Hg–S coordination geometries, the prevalence of close intramolecular Hg $\cdots$ S, Hg $\cdots$ O and Hg $\cdots$ N interactions notwithstanding.

**Keywords:** Hg $\cdots$ S contacts; supramolecular chemistry; secondary-bonding; coordination polymers; crystal structures



**Citation:** Tiekink, E.R.T. Supramolecular Association via Hg $\cdots$ S Secondary-Bonding Interactions in Crystals of Organomercury(II) Species: A Survey of the Cambridge Structure Database. *Crystals* **2023**, *13*, 385. <https://doi.org/10.3390/cryst13030385>

Academic Editor: Sławomir Grabowski

Received: 6 February 2023  
Revised: 16 February 2023  
Accepted: 16 February 2023  
Published: 23 February 2023



**Copyright:** © 2023 by the author. Licensee MDPI, Basel, Switzerland. This article is an open access article distributed under the terms and conditions of the Creative Commons Attribution (CC BY) license (<https://creativecommons.org/licenses/by/4.0/>).

## 1. Introduction

Intermolecular interactions between molecules in crystals, such as the Hg $\cdots$ S interactions forming the focus of this bibliographic review of the supramolecular association occurring between organomercury species in their crystals, have traditionally been classified as secondary-bonding interactions [1], building upon the emerging crystallographic literature of molecular packing at that time [2–4]. Very recently, a new term has been proposed for intermolecular interactions involving the zinc-triad elements interacting with an electron-rich species, namely spodium bonding [5]. The emergence of the term spodium bonding is consistent with the plethora of new terms designed to designate the nature of specific intermolecular interactions [6–8].

More specifically, the term spodium bonding relates to the attractive interaction formed between any Group 12 element and an electron-rich species [5], where the Group 12 element exists in the usual +2 oxidation state within a “(pseudo)tetrahedral” environment. As the proposers of this term mentioned in their original work [2], spodium was a term employed in the 13th Century and referred to mixtures of zinc oxide with other metals. Whatever the terminology, Group 12 elements, especially the heavier cadmium and mercury congeners, are well known to form additional interactions in their crystals with a range of donors, for example and relevant to the present study, sulphur, especially when present as a component of 1,1-dithiolate ligands; for example, dithiocarbamate [ $^{-}S_2CNRR'$ ], xanthate [dithiocarbonate;  $^{-}S_2COR$ ] and dithiophosphate [ $^{-}S_2POR(OR')$ ] [9–14]; R,R' = alkyl, aryl. This notwithstanding, it is noted that the term spodium bonding has gained wide acceptance in studies of the supramolecular association of the Group 12 elements [15–19], including theoretical aspects [20–24] and those relevant to protein structures [25]. It has been argued very recently that a more relaxed definition of spodium bonding might be appropriate [26].

Herein, in continuation of on-going bibliographic surveys of the supramolecular assembly patterns featuring chalcogenides interacting with various electron-donors [27–33],

a review of the known organomercury species, generally thiolates, with crystallographically determined structures is presented. For this purpose, structural data were extracted from the Cambridge Structural Database [CSD; [34]] and evaluated by employing a combination of PLATON [35] and DIAMOND [36]. The specific purpose of the study is to highlight the different supramolecular aggregation patterns encompassing Hg $\cdots$ S interactions apparent in the crystals of organomercury species, which are shown to range from zero- to two-dimensional assemblies, to emphasise past systematic studies in the field and to alert readers to the historical recognition of such supramolecular connectivity by a large number of crystallographers over the years.

## 2. Methods

A search of the CSD (version 5.43 + two updates) [34] was conducted by employing the program ConQuest (version 2022.3.0) [37]. The analysis was based on all crystal structures having both a formal Hg–C bond as well an Hg $\cdots$ S contact less than the sum of the van der Waals radii of mercury (1.55 Å) and sulphur (1.80 Å), that is, 3.35 Å, in crystals containing both mercury and sulphur. These are the standard values in the CSD and were employed in order to be consistent with previous surveys. The retrieved structures had to have three-dimensional coordinates based on single-crystal experiments and were non-polymeric. No other criteria were applied. Manual sorting of the 75 “hits” ensued employing both PLATON [35] and DIAMOND [36] to remove structures where the disorder impacted upon the Hg $\cdots$ S contact and instances when the Hg $\cdots$ S contact was obviously operating in concert with another supramolecular synthon. An example of one such structure is shown in Figure 1. Here, [38], the supramolecular association between the interacting species in the co-crystal include cooperating Hg $\cdots$ S and Hg $\cdots$ O contacts. Hence, this example was excluded from the survey. After the manual screening and following the removal of duplicates, there were 62 examples of crystals featuring at least one Hg $\cdots$ S contact. All diagrams included herein are original and were generated with DIAMOND [36].

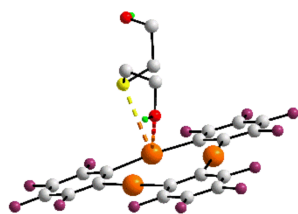


**Figure 1.** Supramolecular association in the crystal comprising tris( $\mu_2$ -perfluoro-*o*-phenylene)-trimercury bis(2-hydroxyethyl)sulphide (1:1) whereby the constituent molecules are assembled into a zero-dimensional aggregate, connected by both Hg $\cdots$ S and Hg $\cdots$ O contacts shown as orange/yellow and orange/red dashed lines, respectively. The colour code for this and subsequent diagrams: orange—mercury; yellow—sulphur; plum—fluoride; red—oxygen; grey—carbon; green—hydrogen. Non-acidic hydrogen atoms are removed for clarity.

## 3. Results and Discussion

The following discussion is broken down to describe representative zero-dimensional aggregation ahead of one-dimensional examples then the smaller number of two-dimensional assemblies. In general, examples among the zero-dimensional aggregates are arranged in order of increasing Hg $\cdots$ S separation for series of closely related compounds featuring common supramolecular synthons. Similar sorting is evident for the smaller number of one-dimensional aggregates which are sorted first, in terms of the topology of the chain. The Supplementary Materials, Figures S1–S62, contain full details of chemical composition, images and extra details, such as additional intramolecular and/or intermolecular contacts, for all aggregates discussed herein. The discussion herein focuses solely on the nature of the Hg $\cdots$ S contacts formed and upon the supramolecular aggregates in which they are found; motivation for the study of the individual compounds and their potential applications,

the interested reader is referred to the original article(s). The survey commences with an overview of molecules assembling into zero-dimensional aggregates.

### 3.1. Zero-Dimensional Aggregates

There are two examples of zero-dimensional aggregates sustained by a single Hg⋯S contact; the key geometric data for these zero-dimensional aggregates are included in Table 1. In the first of these, MeHg(2-aminocyclopent-1-ene-1-carbodithioato) (**1**), two molecules comprise the crystallographic asymmetric-unit and these assemble as shown in Figure 2a [39]. The structure is of dual interest in that (i) if a longer Hg⋯S contact is considered, that is, 3.362(2) Å, the two-molecule aggregates are assembled into a supramolecular chain with a twisted topology (see Supplementary Materials, Figures S1–S37), and (ii) **1** is a rare example herein of having a polymorphic relation, that is, **57**, discussed below. The second example is noted in a 1:2 multi-component crystal related to that shown in Figure 1. In **2** [38], one of the mercury atoms of the tri-mercury molecule accepts an Hg⋯S interaction from the P-bound thione-S atom of one of the two independent dimethyl(4-nitrophenyl)-thiophosphate co-formers, as illustrated in Figure 1b. Indeed, the sulphur straddles the three mercury atoms of the ring but the additional Hg⋯S separations are longer than the chosen van der Waals cut-off, that is, 3.399(3) and 3.428(3) Å. A similar situation pertains to the sulphur atom of the second conformer that sits atop the opposite face with Hg⋯S separations in the range 3.375(3) to 3.651(5) Å. The molecule in **2** represents the first of only three diorganomercury species discussed in this overview, the remaining examples comprise organomercury thiolate derivatives.

**Table 1.** Summary of key geometric parameters (Å, °) for zero-dimensional aggregates 1–20.

| Crystal                | Hg⋯S       | C–S⋯Hg    | X–S⋯Hg       | Y–Hg⋯S       | C–Hg⋯S    | CSD REFCODE | Ref. |
|------------------------|------------|-----------|--------------|--------------|-----------|-------------|------|
| <b>1</b>               | 3.328(3)   | 119.9(3)  | Hg, 97.35(8) | S, 85.76(7)  | 98.3(3)   | IHOLEW      | [39] |
| <b>2</b>               | 3.278(5)   | 86.1(3)   | C, 90.4(3)   | P, 154.3(2)  |           | CEJNUB      | [38] |
| <b>3</b>               | 3.0773(13) | 90.33(16) |              | S, 89.24(4)  | 99.81(13) | FUPFEC      | [40] |
| <b>4</b> <sup>a</sup>  | 3.133(3)   | 92.8(3)   |              | S, 91.01(8)  | 96.7(3)   | FOKBIQ      | [41] |
|                        | 3.191(3)   | 86.7(3)   |              | S, 91.13(8)  | 97.4(3)   |             |      |
| <b>5</b>               | 3.145(2)   | 92.9(3)   |              | S, 90.77(7)  | 95.9(3)   | LUWZOU      | [42] |
| <b>6</b>               | 3.148(8)   | 98.8(8)   |              | S, 90.2(2)   | 96.9(5)   | MEDTHG      | [43] |
| <b>7</b>               | 3.161(5)   | 99.3(6)   |              | S, 92.50(13) | 97.8(5)   | FUPFIG      | [40] |
| <b>8</b>               | 3.1727(13) | 90.01(17) |              | S, 91.81(4)  | 98.17(13) | YOLJAL      | [44] |
| <b>9</b>               | 3.174(3)   | 94.6(4)   |              | S, 89.94(7)  | 99.6(3)   | EKIYUT      | [45] |
| <b>10</b>              | 3.1809(9)  | 93.54(13) |              | S, 90.54(3)  | 97.28(10) | GUVQUJ      | [46] |
| <b>11</b>              | 3.181(3)   | 98.5(4)   |              | S, 93.27(9)  | 95.5(3)   | EKIYON      | [45] |
| <b>12</b>              | 3.191(5)   | 88.8(5)   |              | S, 92.87(13) | 92.1(4)   | FODRUN      | [47] |
| <b>13</b>              | 3.2179(18) | 98.5(2)   |              | S, 94.03(6)  | 93.1(2)   | YOLHUD      | [44] |
| <b>14</b>              | 3.230(2)   | 96.5(3)   |              | S, 92.02(7)  | 96.9(2)   | FUPFAY      | [40] |
| <b>15</b>              | 3.2479(15) | 93.80(18) |              | S, 91.65(4)  | 92.53(14) | NEGRID      | [48] |
| <b>16</b> <sup>a</sup> | 3.251(2)   | 87.8(2)   |              | S, 87.8(7)   | 99.2(2)   | HEGGOS      | [49] |
|                        | 3.341(2)   | 87.1(2)   |              | S, 94.65(6)  | 92.9(2)   |             |      |
| <b>17</b>              | 3.252(4)   | 93.2(6)   |              | S, 92.47(14) | 95.6(5)   | YOMXUV      | [50] |
| <b>18</b>              | 3.2649(15) | 93.67(16) |              | S, 86.99(4)  | 93.45(16) | LAJGOV      | [51] |
| <b>19</b>              | 3.325(6)   |           | P, 93.6(3)   | S, 83.60(17) | 100.4(4)  | YAHFIW      | [52] |
| <b>20</b>              | 3.152(3)   |           | P, 92.88(11) | S, 84.67(8)  | 97.0(3)   | VIHCUK      | [53] |

a—Two independent molecules comprise the crystallographic asymmetric-unit.

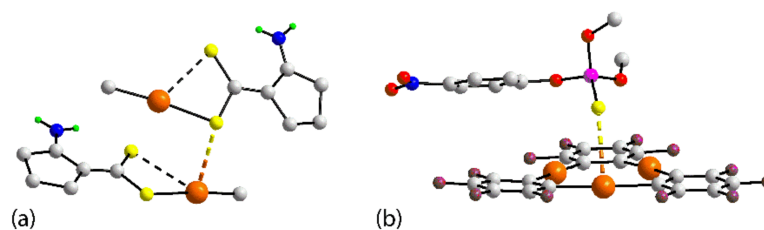


**Figure 2.** Supramolecular association in zero-dimensional aggregates featuring a single Hg...S interaction: (a) **1** and (b) **2**. The black dashed lines in (a) represent intramolecular Hg...S contacts (3.080(2) and 3.163(3) Å). Additional colour code: pink—phosphorus; blue—nitrogen.

Molecule **1** is a relatively rare example of an organomercury(1,1-dithiolate) compound, where the 1,1-dithiolate anion is a cyclopent-1-ene-1-carbodithioato derivative rather than a more common 1,1-dithiolate ligand. There is far greater representation by, in particular, dithiocarbamate 1,1-dithiolate ligands with reduced representation by xanthate and dithiophosphate ligands. Indeed, there are 15 dithiocarbamate derivatives, **3–17**, listed in order of increasing Hg...S separation in Table 1. These are complimented by sole examples each of a xanthate, **18**, a dithiophosphate, **19**, and a dithiophosphinate, **20**; salient geometric data for **18–20** are also collated in Table 1. Except for the methylmercury derivative, MeHg(S<sub>2</sub>CNEt<sub>2</sub>) (**6**), published in 1976 [43], all dithiocarbamate ligands are bound to phenylmercury, therefore have the general formula PhHg(S<sub>2</sub>CNRR'). These are readily classified as symmetric dithiocarbamate ligands, that is, R = R' = Me (**16**), Et (**4**), nPr (**10**) and nBu (**13**); ring dithiocarbamates NRR' = (CH<sub>2</sub>CH<sub>2</sub>)<sub>2</sub>Y for Y = C(H)OH (**5**), O (**8**) and S (**17**); and dissymmetric species where R = CH<sub>2</sub>C<sub>5</sub>H<sub>4</sub>FeC<sub>5</sub>H<sub>5</sub> and R' = iPr (**3**), nBu (**7**), furan-2-ylmethyl (**9**), 4-pyridylmethyl (**11**) and CH<sub>2</sub>Ph (**14**); R = 4-pyridylmethyl and R' = pyrrol-2-yl (**12**); R = CH<sub>2</sub>Ph and R' = furan-2-ylmethyl (**15**). Images for the representatives of each class of compound, that is, **4**, **8** and **7**, are shown in Figure 3.

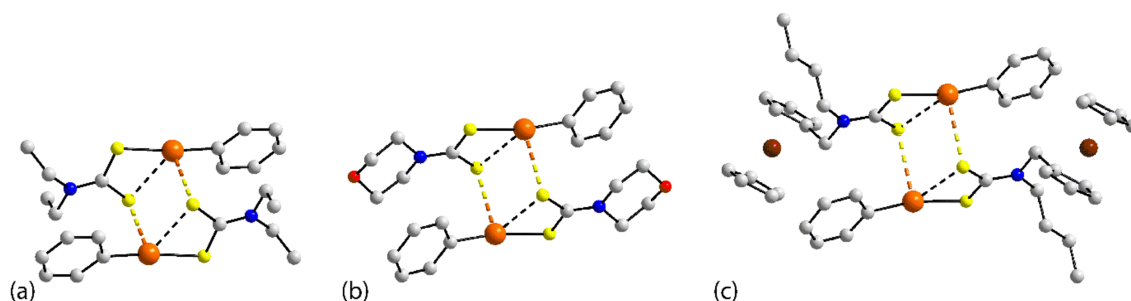


**Figure 3.** Supramolecular association in zero-dimensional aggregates featuring two Hg...S interactions: (a) **4**, (b) **8** and (c) **7**. Additional colour code: brown—iron.

Despite the variety of R and R' substituents, the supramolecular association in the RHg(dithiocarbamate) series is remarkably consistent; crystals **4** and **16** each contain two independent molecules in their respective asymmetric-units. Thus, each aggregate is disposed about a centre of inversion and comprises an eight-membered {...HgSCS}<sub>2</sub> synthon which has the shape of an extended chair. This pertains to **4** where each independent molecule self-associates about a centre of inversion. The exceptional aggregate is noted in **16** whereby the two-independent molecules associate via Hg...S contacts. Within each {...HgSCS}<sub>2</sub> synthon are transannular Hg...S interactions, which correspond to intramolecular Hg...S contacts, arising from the asymmetric mode of coordination by the respective dithiocarbamate ligand. While in all cases the intermolecular Hg...S contact is longer than the intramolecular Hg...S contact, systematic trends are not apparent. Thus, the shortest inter- and intra-molecular Hg...S contacts are found for **3**. The longest intramolecular contact of 3.020(5) Å is noted for **12**. The self-association for the sole methylmercury derivative, **6**, resembles those just described. The skewing in favour of phenylmercury representation

reflects the fact that as opposed to 34 separate X-ray crystal structure determinations for PhHg(dithiocarbamate)s, there is only a single determination for MeHg(dithiocarbamate) recorded in the CSD [34].

To a first approximation, the supramolecular association in the xanthate structure, 4-Me<sub>2</sub>NC<sub>6</sub>H<sub>4</sub>Hg(S<sub>2</sub>COMe) (**18**), Figure 4, having a non-standard mercury-bound organo substituent, resembles those just described for the RHg(dithiocarbamate) series; in this case, reflecting a poorer chelating ability of xanthate compared with dithiocarbamate ligands, the transannular Hg⋯S contact of 3.1128(14) Å is longer than the equivalent interactions for RHg(dithiocarbamate)s. In common with most of the RHg(dithiocarbamate)s and **18**, the remaining aggregates are located about centres of inversion. The common feature of PhHg[S<sub>2</sub>P(OEt)<sub>2</sub>] (**19**) and MeHg(S<sub>2</sub>PPh<sub>2</sub>) (**20**), Figure 4, is the absence of transannular Hg⋯S contacts within the {⋯HgSCS}<sub>2</sub> synthon; that is, Hg⋯S = 3.633(7) and 3.610(3) Å, respectively. This key structural difference reflects the well-documented different chelating versus bridging proclivities of these 1,1-dithiolate ligands [54].

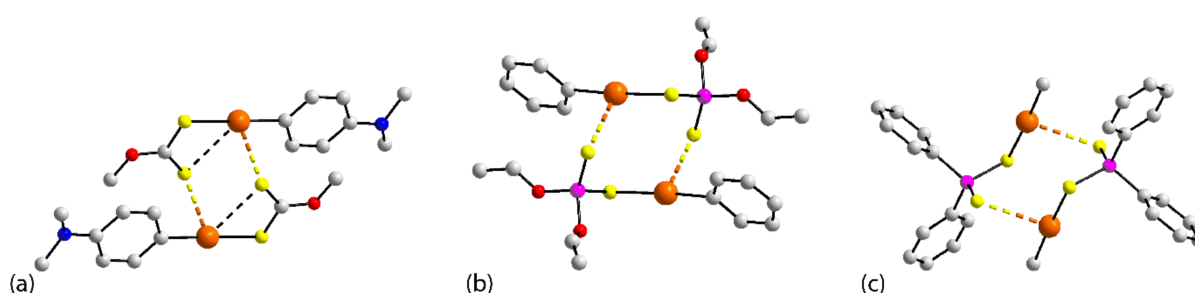


**Figure 4.** Supramolecular association in zero-dimensional aggregates featuring two Hg⋯S interactions: (a) **18**, (b) **19** and (c) **20**.

The next nine supramolecular aggregates to be summarised, that is, **21–29** [55–62], are constructed about a four-membered {⋯HgS}<sub>2</sub> synthon; data, arranged in order of increasing Hg⋯S separation are collated in Table 2. All {⋯HgS}<sub>2</sub> synthons but that in **23** are located about a centre of inversion. In **23**, two independent molecules comprise the asymmetric-unit and these molecules associate to form a two-molecule aggregate; each of the two independent molecules in **25** self-associate about an inversion centre. While a common feature of the majority of structures is the presence of additional, weakly coordinating atoms, two examples are devoid of these, that is, **25** and **26**, Figure 5a.

**Table 2.** Summary of geometric parameters (Å, °) for **21–29**, each featuring a {⋯HgS}<sub>2</sub> synthon in their crystal.

| Crystal                | Hg⋯S       | C–S⋯Hg     | Hg–S⋯Hg    | S–Hg⋯S    | C–Hg⋯S     | CSD REFCODE | Ref. |
|------------------------|------------|------------|------------|-----------|------------|-------------|------|
| <b>21</b>              | 3.224(2)   | 127.7(2)   | 94.55(5)   | 85.45(6)  | 94.91(19)  | BEBLUP      | [55] |
| <b>22</b>              | 3.2498(11) | 142.26(12) | 103.08(3)  | 76.92(3)  | 102.34(19) | VIYLAR      | [56] |
| <b>23</b> <sup>a</sup> | 3.250(2)   | 148.0(3)   | 90.33(6)   | 90.61(6)  | 83.4(2)    | BORCIV      | [57] |
|                        | 3.289(2)   | 146.6(3)   | 89.26(6)   | 89.79(6)  | 89.78(19)  |             |      |
| <b>24</b>              | 3.256(2)   | 136.92(2)  | 106.86(7)  | 73.14(6)  | 108.7(3)   | VIYLIZ      | [56] |
| <b>25</b> <sup>a</sup> | 3.257(4)   | 130.3(3)   | 105.61(14) | 74.39(13) | 103.4(6)   | NEFDEH      | [58] |
|                        | 3.321(4)   | 131.2(3)   | 107.25(14) | 72.75(13) | 103.7(4)   |             |      |
| <b>26</b>              | 3.269(4)   | 134.6(4)   | 100.63(13) | 79.37(12) | 104.2(6)   | JETYEM      | [59] |
| <b>27</b>              | 3.2758(11) | 150.17(12) | 102.88(4)  | 77.12(3)  | 88.04(10)  | PAVVOY      | [60] |
| <b>28</b>              | 3.322(4)   | 139.9(4)   | 104.14(11) | 75.86(10) | 101.6(3)   | DOMCAJ01    | [61] |
| <b>29</b>              | 3.3014(11) | 83.54(16)  | 95.98(4)   | 80.02(4)  | 101.51(13) | HUBRON      | [62] |

a—Two independent molecules comprise the crystallographic asymmetric-unit.

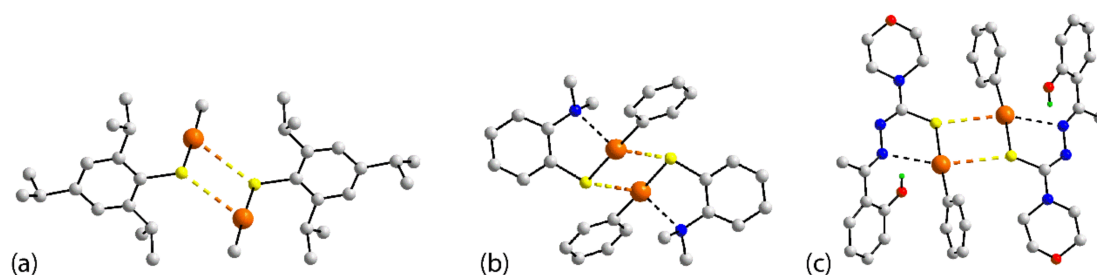


**Figure 5.** Supramolecular association in zero-dimensional aggregates featuring a  $\{\dots\text{HgS}\}_2$  synthon: (a) **26**, (b) **21** and (c) **23**.

In **21**, Figure 5b, molecules self-associate via a  $\{\dots\text{HgS}\}_2$  synthon with a further, weak intramolecular  $\text{Hg}\cdots\text{N}$  interaction [ $d(\text{Hg}\cdots\text{N}) = 2.657(6)$  Å] provided by an amino-N atom of the dimethylamino group occupying the 2-position in the phenylthiolate ligand. This interaction closes a five-membered  $\{\dots\text{HgSC}_2\text{N}\}$  quasi chelate-ring. A similar arrangement is found in the crystal of  $\text{MeHg}(2\text{-pyridylthiolate})$ , **28**, where a four-membered  $\{\dots\text{HgSCN}\}$  ring is formed;  $d(\text{Hg}\cdots\text{N}) = 2.981(9)$  Å. A variation on this theme is noted in the crystal of **23** with a five-membered  $\{\dots\text{HgSCN}_2\}$  quasi chelate-ring linked to a hydrogen-bond-mediated six-membered ring  $\{\dots\text{NC}_3\text{OH}\}$ , Figure 5c;  $d(\text{Hg}\cdots\text{N}) = 2.801(7)$  and  $2.862(7)$  Å. The aggregate in **27**,  $\text{PhHg}[\text{SC}(\text{NH}_2)=\text{NN}=(\text{C}_6\text{H}_{10})]$ , closely resembles that seen in **23**;  $d(\text{Hg}\cdots\text{N}) = 2.526(3)$  Å.

The next two aggregates to be described are closely related. In the crystal of **22**, the  $\{\dots\text{HgS}\}_2$  synthon is complemented by exocyclic, intramolecular  $\text{Hg}\cdots\text{O}$  contacts [ $d(\text{Hg}\cdots\text{O}) = 2.712(4)$  Å] leading to a six-membered  $\{\dots\text{HgSC}_2\text{PO}\}$  quasi chelate-ring, Figure 6a. The phosphaneoxide-O atom is also hydrogen bonded to a methanol molecule of crystallisation. The molecule in **24** is related to that in **22** in that one of the phenyl groups of the phosphane ligand of the latter is further substituted with a second phenylthiolate ligand which also coordinates to an ethylmercury moiety to yield the tetra-nuclear mercury species shown in Figure 6b. The exocyclic mercury atoms also engage in intramolecular  $\text{Hg}\cdots\text{O}$  contacts so the phosphaneoxide-O atom is weakly coordinated to two mercury atoms.

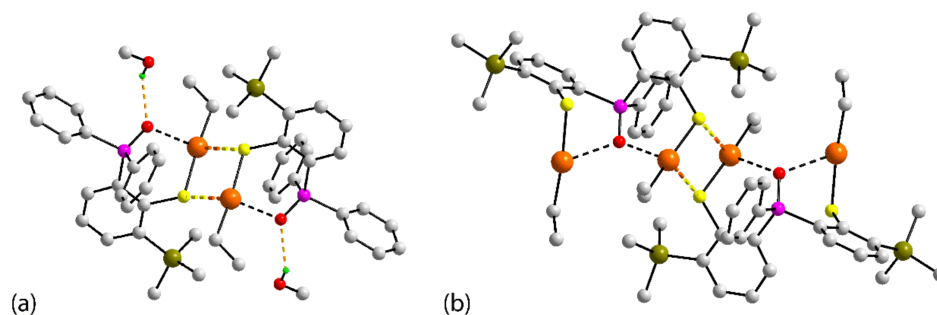


**Figure 6.** Supramolecular association in zero-dimensional aggregates featuring a  $\{\dots\text{HgS}\}_2$  synthon: (a) **22** and (b) **24**. The intramolecular  $\text{Hg}\cdots\text{O}$  contacts are indicated by black dashed lines and the  $\text{O}-\text{H}\cdots\text{O}$  hydrogen bonds are shown as orange dashed lines. Additional colour code: dark-yellow—silicon.

The last aggregate to be described in this category, **29**, is also a tetra-nuclear mercury species, Figure 7a. The 1,2-dithiolate ligand bridges two phenylmercury entities to form a di-nuclear molecule which self-associates to form a centrosymmetric  $\{\dots\text{HgS}\}_2$  synthon. The mercury atom participating in the synthon also forms a weak intramolecular  $\text{Hg}\cdots\text{S}$  contact [ $2.9315(12)$  Å]. Inter-dimer  $\text{Hg}\cdots\text{O}(\text{carbonyl})$  contacts of  $2.738(4)$  Å link the dimers into a linear, supramolecular chain, Figure 7b.

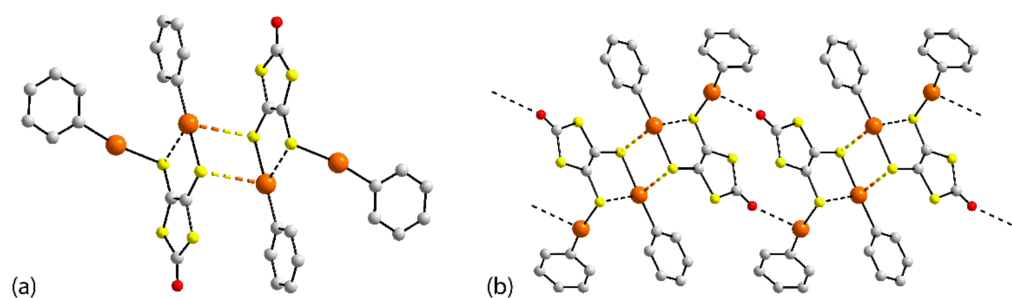


**Figure 7.** Supramolecular association in a zero-dimensional aggregate: **29**, (a) featuring a  $\{\dots\text{HgS}\}_2$  synthon and (b) forming a supramolecular chain in **29** via additional  $\text{Hg}\dots\text{O}$  secondary-bonding interactions (black dashed lines).

The third category of zero-dimensional motifs comprises a miscellaneous grouping of diverse aggregation patterns within two-, four- and up to six-dimensional aggregates; relevant data are presented in Table 3.

**Table 3.** Summary of geometric parameters ( $\text{\AA}$ ,  $^\circ$ ) for **30–37**, each featuring  $\text{Hg}\dots\text{S}$  contacts within zero-dimensional aggregates.

| Crystal                | $\text{Hg}\dots\text{S}$ | $\text{X-S}\dots\text{Hg}$ | $\text{Y-S}\dots\text{Hg}$ | $\text{C-Hg}\dots\text{S}$ | $\text{S-Hg}\dots\text{S}$ | CSD REFCODE | Ref. |
|------------------------|--------------------------|----------------------------|----------------------------|----------------------------|----------------------------|-------------|------|
| <b>30</b>              | 3.206(2)                 | C, 88.1(2)                 | S, 83.05(5)                | 96.7(2)                    |                            | CIJPOB      | [63] |
| <b>31</b>              | 3.2463(15)               | C, 98.29(17)               | S, 83.03(4)                | 93.9(3)                    |                            | CIJPVIV     | [63] |
| <b>32</b>              | 3.2523(6)                | C, 99.88(7)                | S, 84.542(16)              | 93.89(8)                   |                            | CIJQAO      | [63] |
| <b>33</b>              | 3.349(12)                | C, 90(1)                   | Hg, 88.7(3)                | 94(2)                      | 85.9(4)                    | KAPWUT      | [64] |
| <b>34</b>              | 3.348(5)                 | C, 99.9(6)                 |                            | 97.7(4)                    | 82.91(15)                  | FAZBOX      | [65] |
| <b>35</b> <sup>a</sup> | 3.316(8)                 | C, 137(1)                  | Hg, 102.2(2)               | 106(1)                     | 77.8(2)                    | QUGVUJ      | [66] |
|                        | 3.294(8)                 | C, 107(1)                  | Hg, 97.4(2)                | 90(1)                      | 93.1(2)                    |             |      |
| <b>36</b> <sup>a</sup> | 3.2465(15)               | Si, 138.66(7)              | Hg, 95.0(4)                | 97.33(13)                  | 88.83(4)                   | XUYROY      | [67] |
|                        | 3.3737(15)               | Si, 138.23(8)              | Hg, 92.27(4)               | 96.46(13)                  | 83.92(4)                   |             |      |
|                        | 3.2365(16)               | Si, 151.10(8)              | Hg, 104.34(5)              | 95.54(13)                  | 87.11(5)                   |             |      |
| <b>37</b> <sup>b</sup> | 3.306(5)                 | C, 86.3(5)                 | Hg, 95.03(12)              | 97.0(3)                    | 84.97(12)                  | FOKBEM      | [41] |
|                        | 3.329(4)                 | C, 118.3(5)                |                            | 94.7(4)                    | 80.91(13)                  |             |      |
|                        | 3.332(4)                 | C, 86.1(5)                 | Hg, 97.51(13)              | 93.4(4)                    | 85.19(9)                   |             |      |

a—Two independent molecules comprise the crystallographic asymmetric-unit. b—Three independent molecules comprise the crystallographic asymmetric-unit.

The first three aggregates,  $\text{RHg}[\text{tris}(2\text{-mercapto-1-}t\text{-butylimidazolyl})\text{hydroborato}]$ , for  $\text{R} = \text{Me}$  (**30**),  $\text{Me}$  (**31**; tetra-acetonitrile solvate) and  $\text{Et}$  (**32**; hemi-acetone solvate) are notable for two key reasons. From a structural perspective, each molecule aggregates about a centre of inversion forming a 16-membered  $\{\dots\text{HgSCNBNCs}\}_2$  synthon with a distinctive step-like conformation. In each molecule, the third thione-S atom also forms a close, intramolecular contact with mercury, with  $\text{Hg}\dots\text{S}$  separations of 3.347(2), 3.285(2) and 3.318(6)  $\text{\AA}$  for **30–32**, respectively; these are shown as black dashed lines in Figure 8a for **30**. The structural interest notwithstanding, as opposed to most other studies in this area, including crystallographic investigations, which were driven largely by academic curiosity, the focus of this study [63] was upon putative detoxification mechanisms of organomercurials. More specifically, **30–32** formed part of a series of model compounds to emulate an organomercurial lyase, *MerB*, in its ability to cleave  $\text{Hg-C}$  bonds via protonolysis [68].

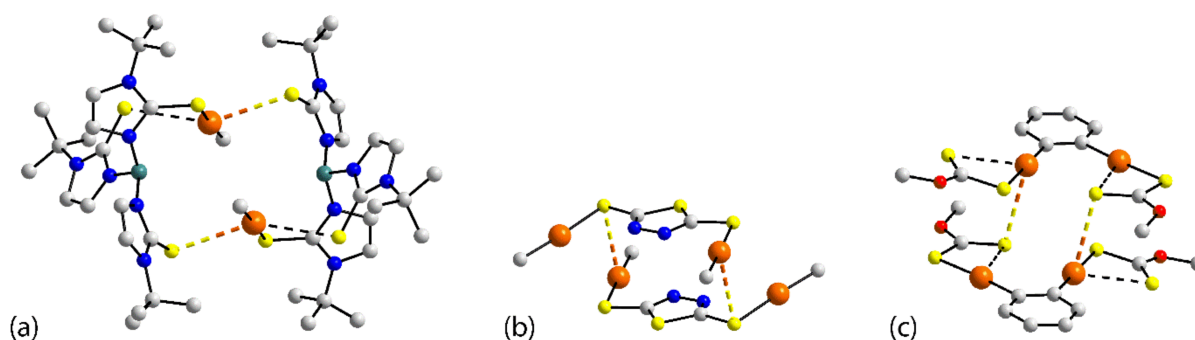


**Figure 8.** Supramolecular association in zero-dimensional aggregates featuring two Hg $\cdots$ S interactions: (a) **30**, (b) **33** and (c) **34**. The intramolecular Hg $\cdots$ S contacts in (a,c) are shown as black dashed lines. Additional colour code: teal—boron.

With a Hg $\cdots$ S separation of 3.349(12) Å right at the limit of the search criteria, the centrosymmetric aggregate in di-nuclear **33** assembles via a 12-membered  $\{\cdots\text{HgSC}_3\text{S}\}_2$  synthon, Figure 8b. The rather long Hg $\cdots$ S distance can be traced to a short intramolecular Hg $\cdots$ N contact of 2.93(3) Å as well as a second Hg $\cdots$ S contact of 3.429(13) Å involving the exocyclic mercury atom. Further inter-dimer Hg $\cdots$ N contacts [2.765(3) Å] assemble molecules into a three-dimensional array. A larger 14-membered  $\{\cdots\text{HgC}_2\text{HgSCS}\}_2$  synthon is noted in the dimeric aggregate of di-nuclear **34**, Figure 8c, where mercury atoms occupy 1,2-positions of a phenyl ring. Intramolecular Hg $\cdots$ S [3.014(6) and 3.151(6) Å] interactions are also noted and further, longer Hg $\cdots$ S contacts [3.354(5) Å] link the dimers into a twisted supramolecular chain (see Supplementary Materials, Figures S1–S37).

A tetra-nuclear aggregate is formed in the crystal of **35** whereby four mono-nuclear molecules assemble via Hg $\cdots$ S interactions. One of the two independent molecules comprising the crystallographic asymmetric-unit assembles about an inversion centre and a  $\{\cdots\text{HgS}\}_2$  synthon (first entry for **35** in Table 3). Two of the second independent molecules are linked external to the ring to form the aggregate shown in Figure 9.

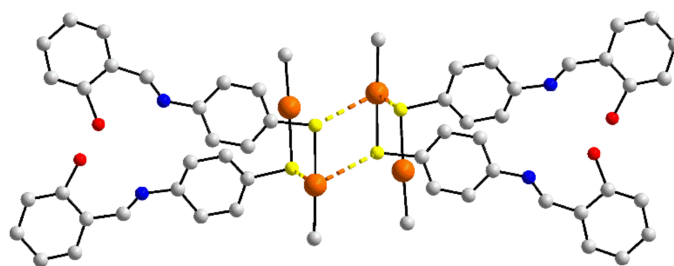


**Figure 9.** Supramolecular association in a zero-dimensional aggregate featuring four Hg $\cdots$ S interactions: **35**. The hydroxyl-H atoms were not located in the original analysis and hence, are not shown.

Two independent molecules also comprise the asymmetric-unit of 4-HO<sub>2</sub>CC<sub>6</sub>H<sub>4</sub>Hg [SSi(OBu-t)<sub>3</sub>] (**36**). Each of these assemble about a site of  $\bar{4}$  to form a tetra-nuclear species. For each tetra-nuclear species, each mercury atom forms a single Hg $\cdots$ S within the sum of the van der Waals radii. However, for the first independent molecule, a second Hg $\cdots$ S contact [3.3737(15) Å], just beyond the sum of the van der Waals radii is apparent giving rise to the distorted cube motif illustrated in the two upper views of Figure 10. The benzoic acid substituents also participate in hydrogen bonding interactions leading to the supramolecular chain shown in the lower view of Figure 10 comprising alternating clusters of each independent molecule.

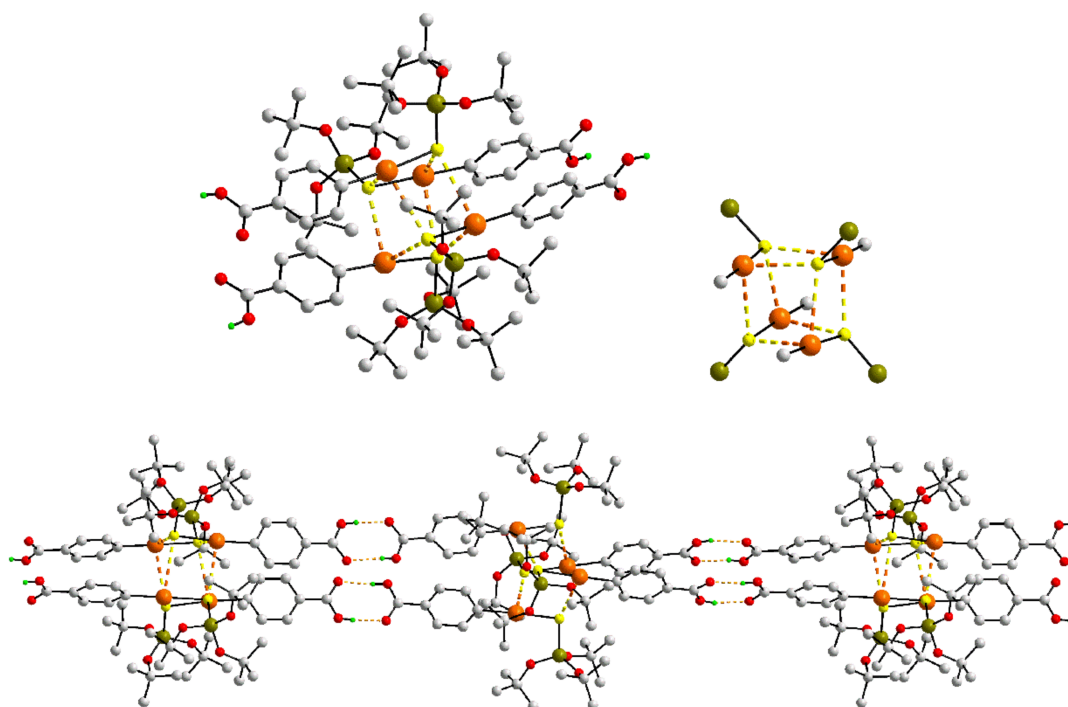


**Figure 10.** Supramolecular associations in **36**: upper view—four-molecule aggregates featuring  $\text{Hg} \cdots \text{S}$  contacts cooperating with an additional four  $\text{Hg} \cdots \text{S}$  contacts beyond the van der Waals radii (right-hand image: simplified view); lower view—supramolecular chain whereby alternating four-molecule aggregates are linked by carboxylate- $\text{O}-\text{H} \cdots \text{O}$ (carbonyl) hydrogen bonding.

The last zero-dimensional aggregate to be described is observed in the crystal of  $\text{PhHg}(\text{S}_2\text{CO}-i\text{-Pr})$  (**37**), a hexa-nuclear species; Figure 11. The asymmetric-unit comprises three independent molecules. One of these self-associates about a centre of inversion to form a two-molecule aggregate resembling the supramolecular association noted for **18** and illustrated in Figure 4a. This aggregate exhibits the shorter of the three intermolecular  $\text{Hg} \cdots \text{S}$  contacts [3.306(5) Å] and a short intramolecular  $\text{Hg} \cdots \text{S}$  contact [3.159(5) Å]. The mercury and sulphur atoms participating in these  $\text{Hg} \cdots \text{S}$  contacts each form an additional  $\text{Hg} \cdots \text{S}$  interaction. Thus, each sulphur atom of the central dimer participates in a second  $\text{Hg} \cdots \text{S}$  interaction [3.332(4) Å] from a pair of second independent molecules with the potential to form a second  $\{\cdots \text{Hg}-\text{S}\}_2$  synthon; however, the second  $\text{Hg} \cdots \text{S}$  separation well exceeds the sum of the van der Waals radii [3.457(3) Å]. At the same time, the mercury atom forms a pair of  $\text{Hg} \cdots \text{S}$  contacts [3.3286(4) Å] with two of the third independent molecules. The result is a six-molecule aggregate. Intramolecular  $\text{Hg} \cdots \text{S}$  interactions are also noted for the second and third independent molecules, being 3.309(4) and 3.211(4) Å, respectively.

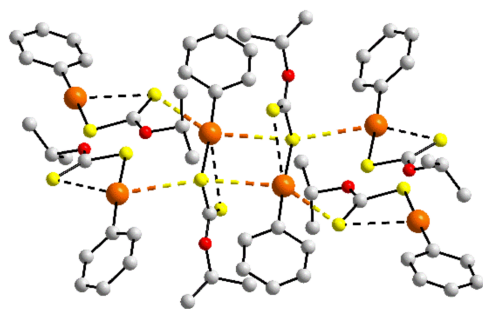


**Figure 11.** Supramolecular association in a zero-dimensional aggregate featuring six  $\text{Hg} \cdots \text{S}$  interactions: **37**.

### 3.2. One-Dimensional Assemblies

In this category, aggregation patterns are arranged in terms of the topology of the resulting one-dimensional chain and in order of the mercury atom content, that is, mono-, di- and tri-nuclear molecules; selected data are collated in Table 4. The first sub-category comprises linear arrays of molecules, **38–41**. The first two one-dimensional aggregates are based on simple linear chains. In PhHg(S<sub>2</sub>PtEt<sub>2</sub>) (**38**), Figure 12, and (Cl<sub>2</sub>C=CCl)Hg(S(C<sub>5</sub>H<sub>4</sub>N-2) (**39**), each mercury atom forms a single Hg⋯S contact. A notable feature of **39** is the formation of short Hg⋯N(pyridyl) contacts [2.808(19) Å]. Decidedly more complicated arrangements are noted in each of **40** and **41**.

**Table 4.** Summary of geometric parameters (Å, °) for **30–37**, each featuring Hg⋯S contacts within one-dimensional aggregates.

| Crystal                | Hg⋯S       | C–S⋯Hg     | X–S⋯Hg            | C–Hg⋯S     | Y–Hg⋯S       | CSD REFCODE | Ref. |
|------------------------|------------|------------|-------------------|------------|--------------|-------------|------|
| <b>38</b>              | 3.182(3)   |            | P, 119.32(2)      | 91.9(4)    | S, 91.12(7)  | LENZIN      | [69] |
| <b>39</b>              | 3.330(7)   | 108.4(8)   | Hg, 89.1(2)       | 98.5(7)    | S, 89.1(2)   | QIQHIH      | [70] |
| <b>40</b> <sup>a</sup> | 3.3247(13) | 128.08(17) | Hg, 90.72(4)      | 99.09(16)  | S, 90.72(4)  | XUHREY      | [71] |
|                        | 3.2613(13) | 112.99(17) | Hg, 90.14(4)      | 94.48(14)  | S, 90.14(4)  |             |      |
|                        | 3.2851(13) | 117.01(17) | Hg, 85.13(4)      | 104.42(14) | S, 71.15(4)  |             |      |
| <b>41</b> <sup>b</sup> | 3.212(6)   | 100.8(7)   | Hg, 112.6(2)      | 93.1(7)    | S, 98.12(19) | WAYPAN      | [72] |
|                        | 3.344(7)   | 104.1(8)   | Hg, 116.4(2)      | 98.0(2)    | S, 91.6(8)   |             |      |
|                        | 3.311(7)   | 100.5(8)   | Hg, 129.4(2)      | 87.0(8)    | S, 97.9(2)   |             |      |
| <b>42</b>              | 3.2929(10) | 100.79(14) | Hg, 81.11(3)      | 86.43(11)  | S, 93.96(3)  | OBIZAC      | [73] |
| <b>43</b>              | 3.293(5)   | 97.5(5)    | Hg,<br>102.31(17) | 92.5(6)    | S, 90.48(16) | NESRUA      | [74] |
| <b>44</b>              | 3.324(11)  | 89.3(8)    | Hg, 117.9(3)      | 92(1)      | S, 91.6(3)   | DOYFIG      | [75] |
| <b>45</b>              | 3.184(7)   | 140.2(6)   | Hg, 92.29(12)     | 97.4(7)    | S, 85.23(16) | QUGVIX      | [66] |
|                        | 3.251(7)   | 132.7(7)   | Hg, 94.59(12)     | 97.8(7)    | S, 83.69(16) |             |      |
|                        | 3.229(5)   | 107.8(7)   | Hg, 109.91(8)     | 95.0(5)    | S, 89.87(13) |             |      |
| <b>46</b>              | 3.226(2)   | 108.6(3)   | Hg, 96.60(7)      | 96.4(3)    | S, 81.75(8)  | DOFNOC      | [76] |
|                        | 3.312(2)   | 145.0(3)   | Hg, 94.79(7)      | 101.9(3)   | S, 79.58(7)  |             |      |
|                        | 3.272(2)   | 108.5(3)   | Hg, 119.07(8)     | 92.6(3)    | S, 89.53(7)  |             |      |
| <b>47</b>              | 3.254(5)   | 92.7(5)    | Hg, 85.66(13)     | 94.7(5)    | S, 93.07(16) | YOMXIJ      | [50] |
| <b>48</b>              | 3.0809(10) | 87.97(13)  | Hg, 109.03(4)     | 94.35(13)  | S, 85.62(3)  | XUHREY01    | [71] |
| <b>49</b>              | 3.183(15)  | 114(1)     | Hg, 102.1(4)      | 100(2)     | S, 86.4(4)   | PHGMSP      | [77] |
| <b>50</b>              | 3.3251(17) | 87.6(2)    | Hg, 133.46(6)     | 101.2(2)   | S, 78.08(5)  | OCOLEY      | [78] |
| <b>51</b>              | 3.290(3)   | 88.6(3)    | Hg, 95.82(7)      | 95.7(3)    | S, 86.23(7)  | LAWTUB      | [79] |
| <b>52</b>              | 3.179(5)   |            | P, 103.6(2)       | 89.0(5)    | C, 91.6(5)   | GILNOE      | [80] |
| <b>53</b>              | 3.296(4)   | 104.2(2)   | Hg,<br>105.28(13) | 96.5(7)    | S, 86.56(15) | CHMEHG      | [81] |
| <b>54</b>              | 3.303(4)   | 83.6(4)    | Hg,<br>114.98(12) | 95.7(4)    | S, 79.66(11) | LOPGUT      | [82] |
| <b>55</b>              | 3.268(3)   | 91.1(4)    |                   | 96.6(3)    | S, 83.52(9)  | FUPFOM      | [40] |
|                        | 3.303(3)   | 91.7(4)    |                   | 95.4(3)    | S, 84.37(9)  |             |      |
| <b>56</b>              | 3.249(11)  | 100.7(3)   | Hg, 93.99(18)     | 92.1(7)    | S, 89.40(18) | CECWOW      | [83] |

Table 4. Cont.

| Crystal         | Hg...S     | C-S...Hg   | X-S...Hg          | C-Hg...S     | Y-Hg...S     | CSD REFCODE | Ref. |
|-----------------|------------|------------|-------------------|--------------|--------------|-------------|------|
| 57              | 3.350(6)   | 102.3(2)   | Hg, 95.6(2)       | 94.0(7)      | S, 87.74(18) | IHOLEW01    | [39] |
|                 | 3.1797(17) | 94.64(15)  |                   | 96.72(17)    | S, 90.45(4)  |             |      |
|                 | 3.3501(12) | 145.95(16) | Hg, 111.66(4)     | 105.81(17)   | S, 68.34(4)  |             |      |
| 58 <sup>b</sup> | 3.240(3)   | 131.4(4)   | Hg, 95.18(10)     | 96.3(5)      | S, 84.82(10) | QUGVOD      | [66] |
|                 | 3.251(3)   | 131.3(4)   | Hg, 91.80(11)     | 93.5(4)      | S, 88.20(11) |             |      |
|                 | 3.128(3)   | 111.9(4)   | Hg,<br>106.76(11) | 92.8(5)      | S, 88.27(10) |             |      |
| 59              | 3.160(3)   | 107.3(4)   | Hg,<br>108.01(11) | 93.1(4)      | S, 87.11(10) | DOFNIW      | [75] |
|                 | 3.2491(14) | 127.22(17) | Hg, 96.07(5)      | 97.3(2)      | S, 83.93(4)  |             |      |
|                 | 3.2406(13) | 109.2(2)   | Hg, 104.36(5)     | S, 94.80(19) | S, 88.65(4)  |             |      |

a—Four independent molecules comprise the crystallographic asymmetric-unit. b—Two independent molecules comprise the crystallographic asymmetric-unit.

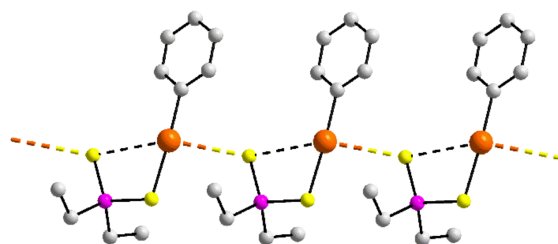
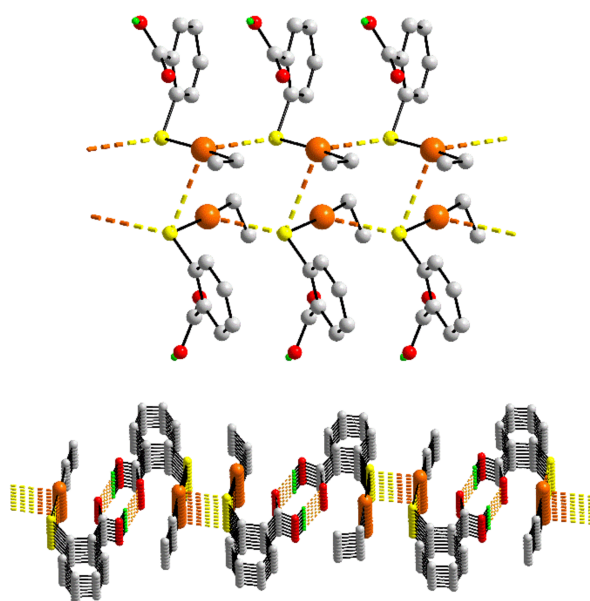


Figure 12. Supramolecular association in a one-dimensional aggregate featuring Hg...S interactions: 38.

EtHg[SC<sub>6</sub>H<sub>4</sub>(CO<sub>2</sub>H)-2] (**40**) attracted interest in terms of the “Thimerosal controversy” concerning the relationship between the use of EtHg[SC<sub>6</sub>H<sub>4</sub>(CO<sub>2</sub>H)-2] as a preservative in vaccines which was said to be, but not substantiated, as the causative agent of autism in children [84]. In terms of the solid-state, four crystallographically independent molecules comprise the asymmetric-unit of **40**. Each of these assembles into a linear, supramolecular via a single Hg...S interaction. As illustrated in the top view of Figure 13, two chains associate via an additional Hg...S interaction to form a supramolecular tape resembling a ladder. Data corresponding to one such assembly is presented in Table 4; the staves correspond to the third entry (for **40** in Table 4). For the second pair of linear chains, the Hg...S distance corresponding to the staff is slightly beyond the standard van der Waals separation; see Supplementary Materials, Figures S38–S59 for data. Intramolecular Hg...O(carbonyl) interactions are also observed with separations in the range 2.872(4) to 2.901(4) Å.

Further supramolecular association is noted in the crystal of **40** through the formation of eight-membered {...HOCO}<sub>2</sub> synthons arising from carboxylic acid–O–H...O(carbonyl) hydrogen bonding. This results in a supramolecular layer as illustrated in the lower view of Figure 13. Finally, it is noted that **40** is a polymorph of **48**, as discussed below.

The molecule in **41** is tri-nuclear MeC(CH<sub>2</sub>SHgMe)<sub>3</sub>; the molecule lacks symmetry. The asymmetric-unit contains two independent molecules indicating there are six independent mercury atoms in the crystal of **41**. Despite this, only two mercury atoms engage in Hg...S interactions. Each independent molecule self-associates into a linear chain (entries 1 and 2 for **41** in Table 4) and, as for **40**, the two chains are connected via an additional Hg...S contact (entry 3 for **41** in Table 4) to form the one-dimensional assembly illustrated in Figure 14. The additional Hg...S contact involves the mercury atom already participating in a Hg...S interaction indicating this atom forms two Hg...S contacts.



**Figure 13.** Supramolecular association in the crystal of **40**: upper view—a one-dimensional aggregate with a ladder topology featuring three independent Hg...S interactions; lower view—side-on view of the supramolecular layer formed through the agency of carboxylic acid-O-H...O(carbonyl) hydrogen bonding and {...HOCO}<sub>2</sub> synthons. Here, the chains of the upper view are connected into a two-dimensional assembly via the hydrogen bonding (non-participating hydrogen atoms are omitted).

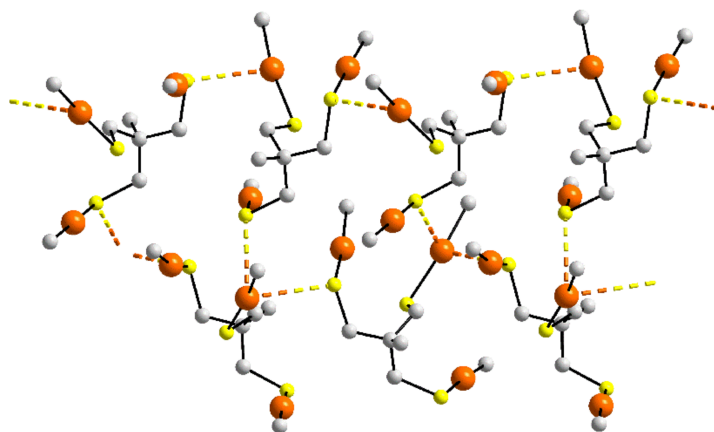


**Figure 14.** Supramolecular association in a one-dimensional aggregate featuring three Hg...S interactions per trinuclear molecule: **41**.

Molecules in **42–47** assemble into zigzag chains. The simplest example among the series, formulated as PhHg[SC(N=NC<sub>6</sub>H<sub>4</sub>OMe-2)NN(H)C<sub>6</sub>H<sub>4</sub>OMe-2] (**42**), has the zigzag chain propagated along a crystallographic glide axis. In each of **43**, MeHg(Benzylidene-N,N-dimethylcarbamohydrazonothioato) and **44**, MeHg(2-mercapto-4-methylpyrimidinato), similar symmetry prevails leading to the zigzag chain illustrated for **44** in the upper view of Figure 15. The crystal is particularly noteworthy for the presence of mercuriphilic interactions [85]. As highlighted in the lower view of Figure 15, Hg...Hg contacts [3.805(3) Å] link the zigzag chains into double chains. Intramolecular Hg...N contacts are noted in each of **42** [2.725(3) Å], **43** [2.603(16) Å] and **44** [3.02(6) Å].

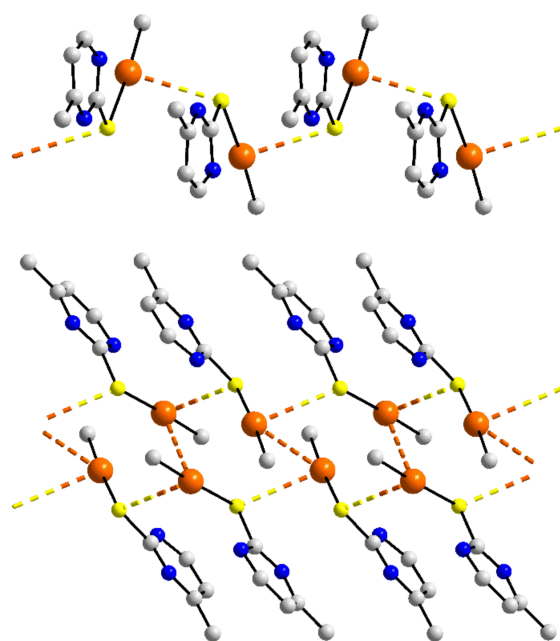


**Figure 15.** Supramolecular association in the crystal of **44**: upper view—zigzag chain featuring Hg $\cdots$ S interactions; lower view—double chain formation through the agency of Hg $\cdots$ Hg interactions shown as orange dashed lines.

The molecules in PhHg(SC<sub>6</sub>H<sub>4</sub>NH<sub>2</sub>-3) (**45**), Figure 16, and PhHg(SPh) (**46**) assemble in an analogous fashion, and each have two independent molecules in the asymmetric-unit. The two independent molecules in **45** assemble via a pair of Hg $\cdots$ S interactions (entries 1 and 2 for **45** in Table 4) leading to a non-symmetric { $\cdots$ HgS}<sub>2</sub> synthon. The dimeric units thus formed are assembled into a zigzag chain with a third Hg $\cdots$ S interaction between them (entry 3 for **45** in Table 4), indicating that one mercury and one sulphur atom form two such contacts.

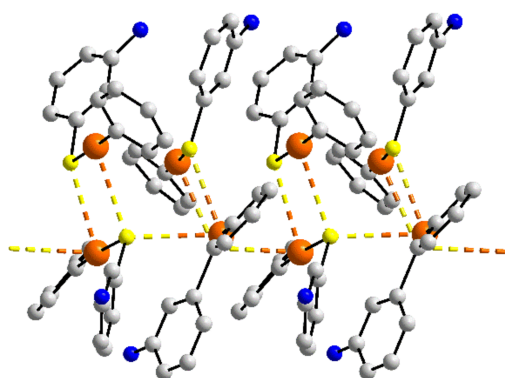


**Figure 16.** Supramolecular association in a zigzag chain in **45** featuring three independent Hg $\cdots$ S interactions. The amino-H atoms were not located in the original study and hence, are not shown.

The di-nuclear molecule in phenylmercury derivative **47** features a bridging dithiocarbamate ligand formulated as {<sup>-</sup>S<sub>2</sub>CN(CH<sub>2</sub>-furan-2)[1,4-CH<sub>2</sub>C<sub>6</sub>H<sub>4</sub>CH<sub>2</sub>](2-furan-2-yl-CH<sub>2</sub>)NCS<sub>2</sub><sup>-</sup>}. Each end of the molecule associates about a 2-fold axis resembling the aggregate shown for **4** in Figure 3a. The di-nuclear molecules are assembled into a zigzag chain through the application of glide symmetry to give the assembly shown in Figure 17. The intramolecular Hg $\cdots$ S interaction is 2.933(8) Å.

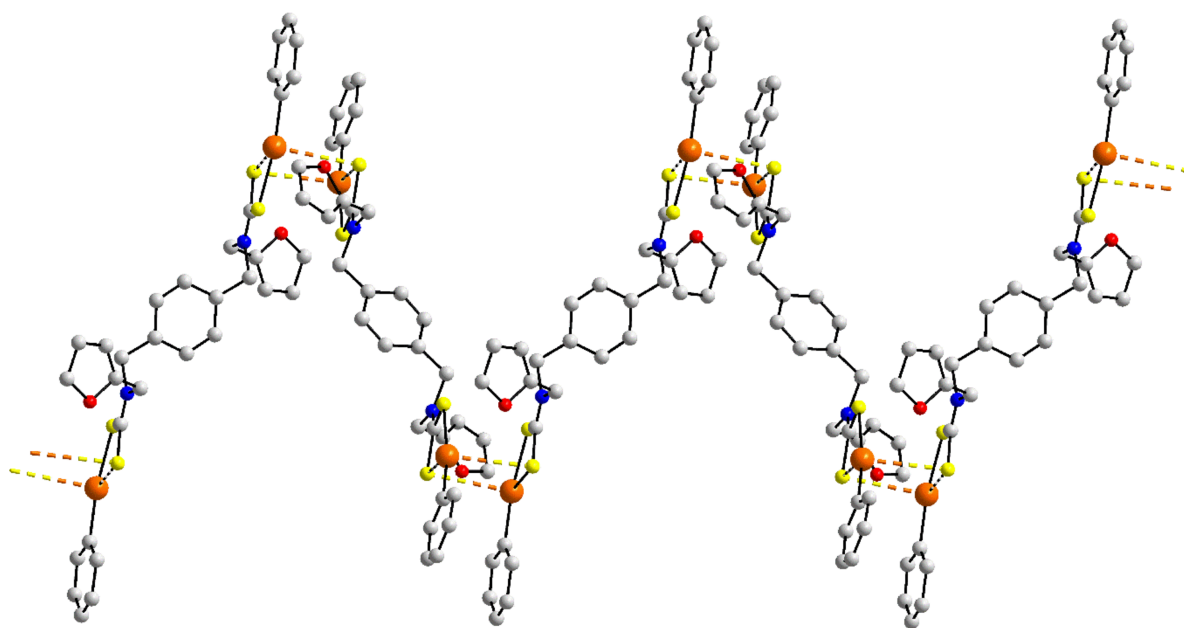


**Figure 17.** Supramolecular association in a zigzag chain in di-nuclear **47**.

The most represented topology among the one-dimensional aggregation patterns to be described is helical, with eight examples. A representative molecule of the relatively straightforward helical chains in each of **48–51** is that in  $\text{EtHg}(\text{SC}_6\text{H}_4(\text{CO}_2\text{H})\text{-}2)$  (**48**). The helical chain featuring  $\text{Hg}\cdots\text{S}$  interactions between molecules is illustrated in Figure 18. The helical chains assemble into a supramolecular layer, being connected by carboxylic acid– $\text{O}-\text{H}\cdots\text{O}(\text{carbonyl})$  hydrogen bonding. The crystal of **48** is a polymorph of **40**, Figure 13, which assembles into a supramolecular tape as each mercury atom forms two  $\text{Hg}\cdots\text{S}$  contacts. Another difference between the polymorphs relates to the absence of intramolecular  $\text{Hg}\cdots\text{O}(\text{carbonyl})$  interactions which are evident in **40**.

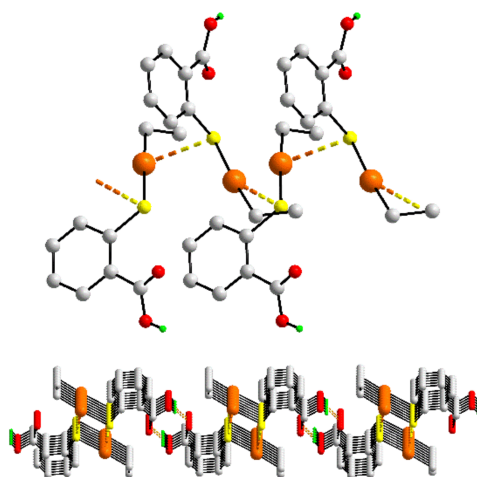


**Figure 18.** Supramolecular association in the crystal of **48**: upper view—a one-dimensional aggregate with a helical topology and featuring  $\text{Hg}\cdots\text{S}$  interactions; lower view—supramolecular layer formed through carboxylic acid– $\text{O}-\text{H}\cdots\text{O}(\text{carbonyl})$  hydrogen bonding. Here, the chains of the upper view are connected into a two-dimensional assembly via hydrogen bonding (non-participating hydrogen atoms are omitted).

The supramolecular aggregation via  $\text{Hg}\cdots\text{S}$  interactions in  $\text{PhHg}(\text{SC}_6\text{H}_3\text{Me-}2,6)$  (**49**),  $\text{MeHg}(4,5\text{-diphenyl-}(1,2,4)\text{triazine-}3\text{-thionato})$  (**50**) and  $\text{MeHg}(\text{phenylmethanethiolato})$  (**51**)

is similar, each being propagated by  $2_1$  screw symmetry as for **48**. In **50**, intramolecular Hg $\cdots$ N contacts of 3.146(5) Å are noted.

In the second of only three examples of a diorganomercury species included in this survey, the Hg[CH<sub>2</sub>P(S)Ph<sub>2</sub>]<sub>2</sub> molecule in **52** is especially noteworthy. The mercury atom is located on a 2-fold axis of symmetry. The molecules assemble into helical chains with two Hg $\cdots$ S contacts per molecule leading to the formation of eight-membered { $\cdots$ HgCPS}<sub>2</sub> synthons, Figure 19. The { $\cdots$ HgCPS}<sub>2</sub> synthons have distinctive chair conformations whereby one each of the P–C bonds lies above and below the plane defined by the Hg<sub>2</sub>S<sub>2</sub> atoms.

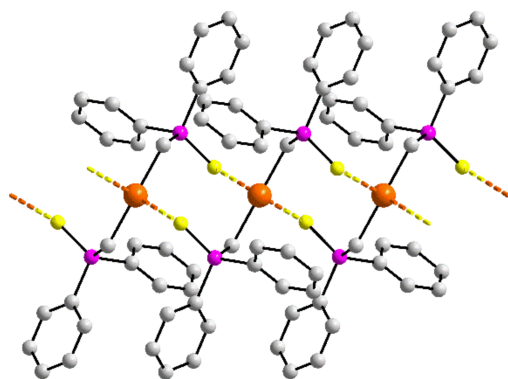


**Figure 19.** Supramolecular association in the crystal of **52**: one-dimensional chain with a helical topology and featuring two Hg $\cdots$ S interactions per mercury atom.

The next three examples in this sub-category relate to supramolecular association between di-nuclear species. The common feature of (MeHg)<sub>2</sub>(S<sub>2</sub>C<sub>6</sub>H<sub>10</sub>) (**53**), Figure 20a, and (PhHg)<sub>2</sub>( $\mu_2$ -2,4-pyrimidinedithiolato) (**54**) is that only one of the two mercury atoms participate in Hg $\cdots$ S interactions within a helical chain. As evident from Figure 20a, intramolecular Hg $\cdots$ S interactions [2.853(16) Å] are present. In **54**, intramolecular Hg $\cdots$ N contacts of 2.774(11) Å are noted.

The molecule in **55** is closely related to that in phenylmercury dithiocarbamate derivative **46** except that the second substituent on the dithiocarbamate ligand is methylene(ferrocenyl) rather than methylene(furanyl-2). The bridging ligand in **55** is non-symmetric but each mercury atom forms chemically equivalent Hg $\cdots$ S interactions, being linked to a molecule within a helical chain to form the assembly shown in Figure 20b. As usual, an intramolecular Hg $\cdots$ S contact is formed by the non-coordinating sulphur atom in each residue [2.877(3) and 2.882(3) Å].

The next two supramolecular chains adopt twisted conformations. Each of the molecules in **56** and **57** comprise mono-nuclear molecules, formulated as PhHg(8-mercaptoquinolinato) and MeHg(2-aminocyclopent-1-ene-1-carbodithioato), respectively. Figure 21a shows the twisted chain in **56**, where the close Hg $\cdots$ N interactions for each independent molecule [ $2 \times 2.46(2)$  Å] are consistent with the strong chelating ability of the 8-mercaptoquinolinato ligand. A supramolecular tape is observed in the crystal of **57**, Figure 21b. The molecule associates about a centre of inversion, forming the shorter of the Hg $\cdots$ S distances. The tape arises through the formation of a second intermolecular Hg $\cdots$ S contact so that the mercury atom forms two Hg $\cdots$ S contacts. As highlighted in Figure 21b, the tape comprises an alternating sequence of four-membered { $\cdots$ HgS}<sub>2</sub> and eight-membered, { $\cdots$ HgSCS}<sub>2</sub> synthons. The intramolecular Hg $\cdots$ S contact distance is 3.1747(11) Å. The structure of **57** represents a second polymorph for MeHg(2-aminocyclopent-1-ene-1-carbodithioato), the first being **1**, a two-molecule aggregate connected by a single Hg $\cdots$ S contact, Figure 2a.

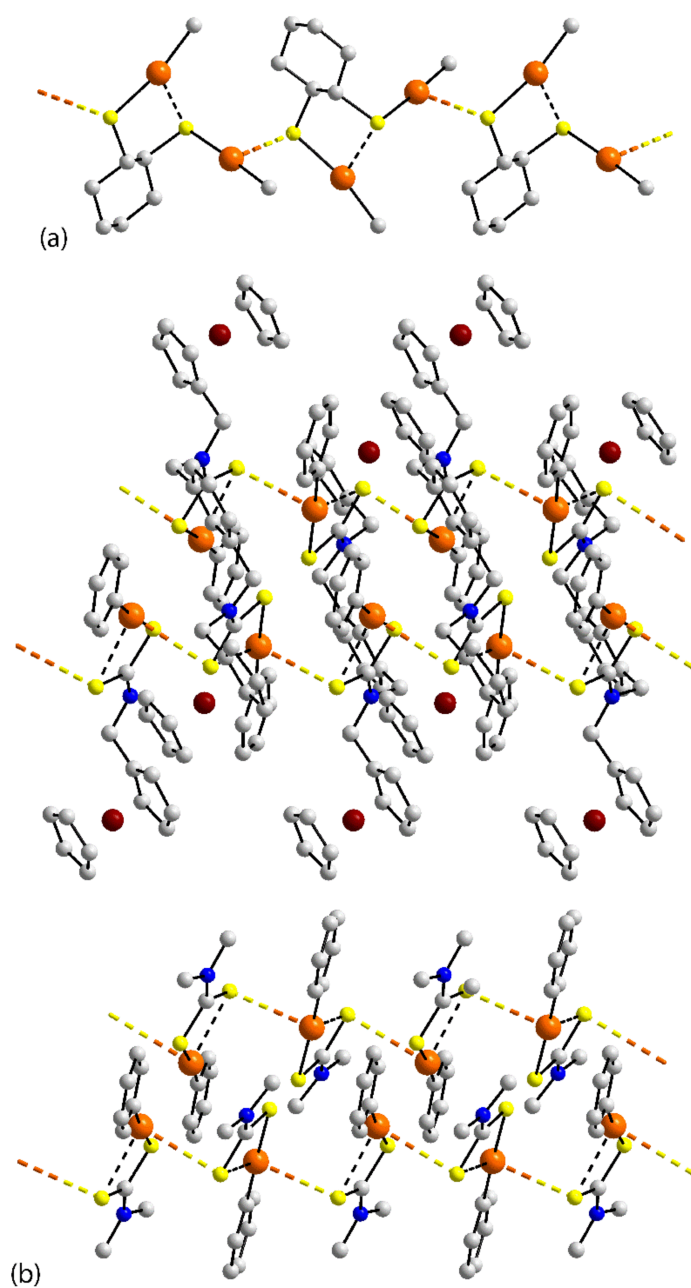


**Figure 20.** Supramolecular association in the crystals with chains having a helical topology: (a) di-nuclear **53** and (b) di-nuclear **55** with the lower view showing only the carbon atoms directly bonded to nitrogen so the links between the chains are absent.

The remaining two one-dimensional aggregation patterns to be described are based on a distinctive square-wave topology, as illustrated for MeHg [3-(2-hydroxybenzylideneamino) phenylthiolato] (**58**) in Figure 22. Two independent molecules comprise the asymmetric-unit of **58** and each of these assembles into a dimeric aggregate across an inversion centre (entries 1 and 2 for **58** in Table 4). These are connected via shorter Hg $\cdots$ S interactions. A similar arrangement is observed for MeHg(SPh) (**59**).

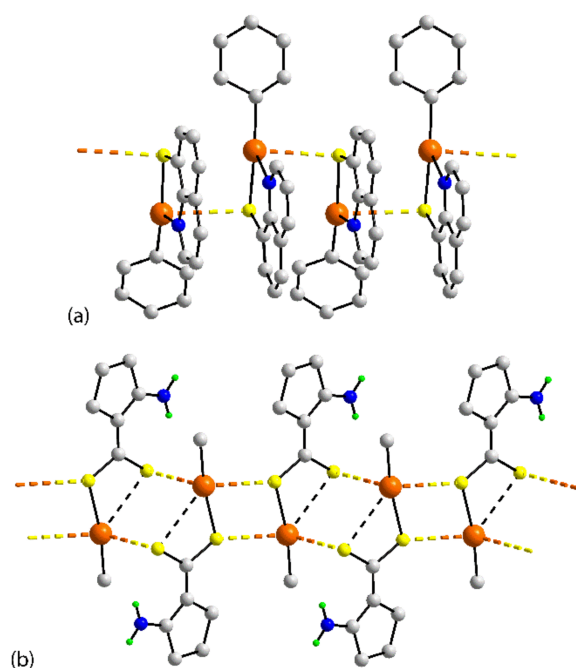


**Figure 21.** Supramolecular association in the crystals with twisted one-dimensional aggregation encompassing Hg $\cdots$ S interactions: (a) di-nuclear **56** and (b) di-nuclear **57**.

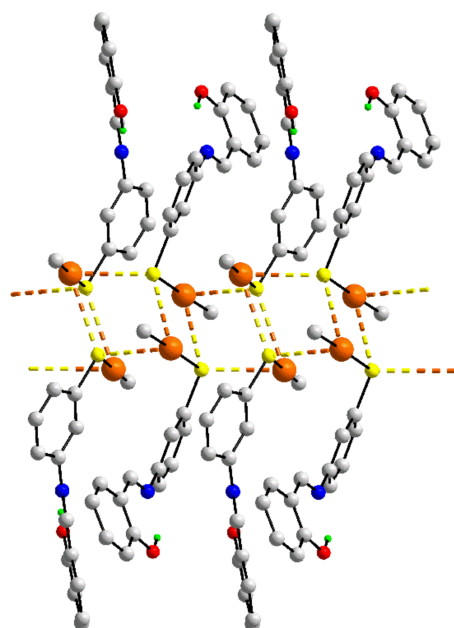


**Figure 22.** Supramolecular association in the crystal of **58**, having a square-wave arrangement of Hg $\cdots$ S interactions within the one-dimensional chain.

### 3.3. Two-Dimensional Assemblies

The three assemblies remaining to be described show Hg $\cdots$ S interactions being pivotal in assembling molecules/aggregates into two-dimensional arrays, see Table 5 for data. In PhMe(2-aminocyclopent-1-ene-1-carbodithioato) (**60**), as opposed to the zero-dimensional aggregation patterns in polymorphic methylmercury analogues **1**, Figure 2a, and **57**, Figure 21b, molecules assemble into a two-dimensional array in which Hg $\cdots$ S interactions play a prominent role. In the crystal and as illustrated in Figure 23, the mercury atom forms two Hg $\cdots$ S contacts with two different molecules so a hexagonal arrangement is evident, comprising an alternating sequence of mercury and sulphur atoms, incorporating

two intramolecular and four intermolecular Hg...S contacts. The intramolecular Hg...S contact has Hg...S = 3.1286(10) Å.

**Table 5.** Summary of geometric parameters (Å, °) for 60–62, each featuring Hg...S contacts within two-dimensional arrays.

| Crystal | Hg...S     | X-S...Hg      | Y-S...Hg      | C-Hg...S   | Z-Hg...S     | CSD REFCODE | Ref. |
|---------|------------|---------------|---------------|------------|--------------|-------------|------|
| 60      | 3.1834(11) |               | C, 98.61(13)  | 90.88(12)  | 93.66(3)     | IHOLIA      | [39] |
|         | 3.2269(10) |               | C, 102.17(12) | 101.38(10) | 81.60(3)     |             |      |
| 61      | 3.203(5)   |               | C, 122.7(7)   | 79.0(2)    | C, 100.5(5)  | EBUSIF      | [86] |
| 62      | 3.2960(12) | Ni, 109.33(4) | P, 165.54(7)  | 88.58(17)  | S, 177.17(3) | COCJUC      | [87] |
|         |            |               |               | 91.42(17)  |              |             |      |

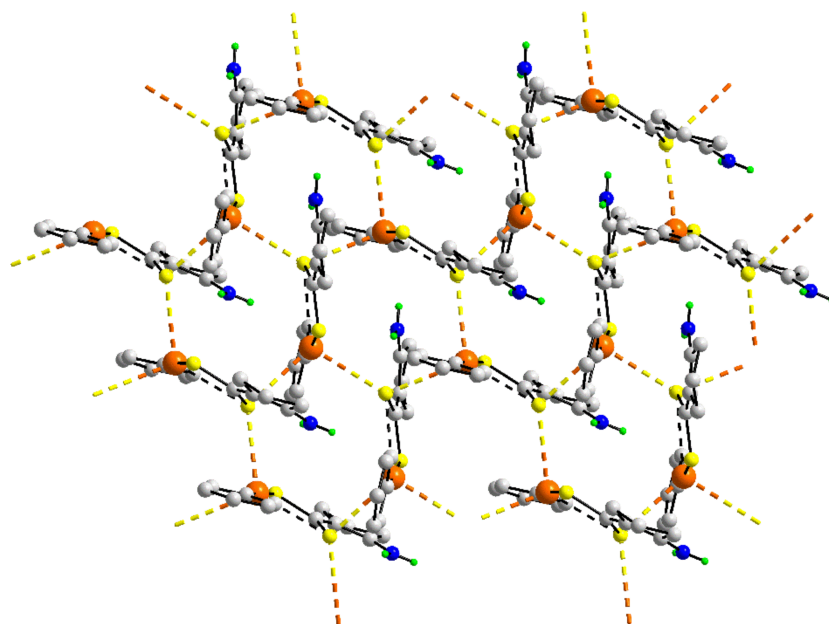


**Figure 23.** Supramolecular layer in the crystal of 60, having a hexagonal pattern of Hg<sub>3</sub>S<sub>3</sub> atoms participating in inter- and intra-molecular Hg...S interactions.

In 61, PhHg[S<sub>2</sub>CN(CH<sub>2</sub>Ph)CH<sub>2</sub>C<sub>5</sub>H<sub>4</sub>N-4], the dithiocarbamate ligand is functionalised with a 4-pyridyl residue; the structural chemistry of such dithiocarbamate ligands has recently been reviewed [88]. In the crystal, a linear chain is formed whereby in addition to the C-, S- donor set, the mercury atom is coordinated intermolecularly by the pyridyl-N atom [Hg...N = 2.74(2) Å]. The supramolecular chains are connected into a two-dimensional array via Hg...S contacts [Hg...S = 3.203(5) Å], as indicated in Figure 24. A side-on view of the supramolecular layer shows the benzyl substituents lie to either side; see Supplementary Materials Figures S61 and S62. In common with all other organomercury dithiocarbamates described herein, an intramolecular Hg...S contact is apparent [Hg...S = 2.993(5) Å].

The last aggregation pattern to be described is found in the crystal of heterometallic species, 62, being only the second diorganomercury species to be described in this survey. Here, molecules of Hg(C<sub>5</sub>H<sub>4</sub>N-4)<sub>2</sub> function as bipyridyl-like molecules, linking two molecules of Ni[S<sub>2</sub>P(O-*i*-Pr)<sub>2</sub>]<sub>2</sub>, leading to extended 2 + 4, trans-N<sub>2</sub>S<sub>4</sub> coordination geometry for nickel(II). The molecules are assembled into a linear supramolecular chain; each of the heavy atoms are situated on a 2-fold axis of symmetry. The chains are assembled by Hg...S interactions into a flat, two-dimensional array with the appearance of a rectangular grid, as shown in Figure 25.

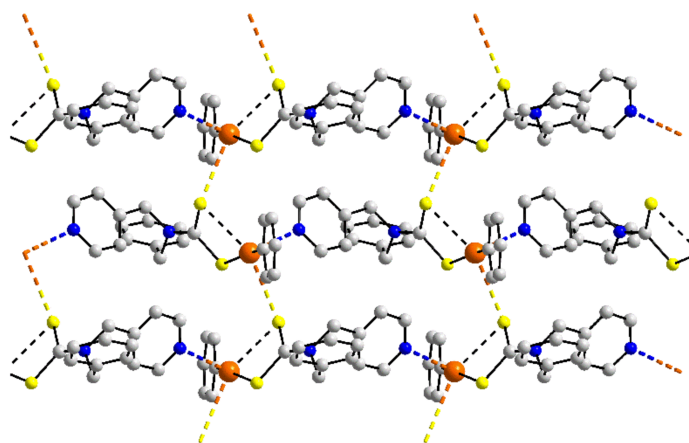


**Figure 24.** Supramolecular layer in the crystal of **61** whereby a linear coordination polymer is linked into a two-dimensional array by Hg...S interactions.

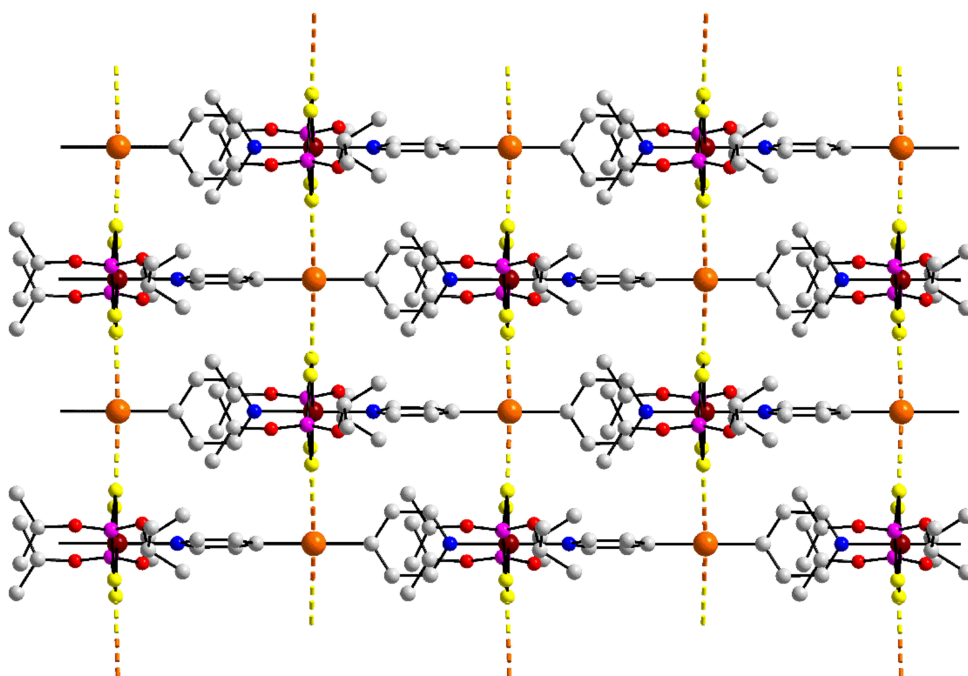


**Figure 25.** Supramolecular layer in the crystal of **62** whereby a heterometallic coordination polymer is linked into a two-dimensional array by Hg...S interactions.

#### 4. Overview

While the first report of intermolecular Hg...S interaction being important in contributing to molecular packing was in 1976 [43], from the foregoing, it is clear that Hg...S interactions play a pivotal role in assembling organomercury species in their crystals, with 62 examples of crystals featuring intermolecular Hg...S interactions. Thus, zero-, one- and two-dimensional aggregation have been described with the majority being either zero- or one-dimensional, that is, 37 and 22 examples, respectively. Of the zero-dimensional aggregates, the majority contain two mercury atoms assembling via eight-membered  $\{\cdots\text{HgSCS}\}_2$  or closely related synthons where the carbon atom is replaced by phosphorus (18), or four-membered  $\{\cdots\text{HgS}\}_2$  synthons (11) although exceptions are noted. Tetra- and hexa-mercury aggregates were observed. A large variety of one-dimensional topologies were noted, that is, linear (4), zigzag (6), helical (8), twisted (2) and step-ladder (2). Most mercury atoms form a single Hg...S interaction but there are a few exceptions.

As has been noted elsewhere, it is rather futile to attempt to correlate weak intermolecular interactions with any geometric parameter [89,90] owing to the decisive but not

quantifiable influence of other factors, such as the nature of other chemical entities, other intra- and inter-molecular interactions, experimental conditions, etc. For the record, the shortest Hg...S separation of 3.0773(13) Å, which corresponds to 92% of the van der Waals separation, was noted in the aggregate described for **3** and the longest was at the limit of the sum of the van der Waals radii, for example **36**. For completeness of the descriptions of a number of aggregates, several other contacts were noted above where the Hg...S separation was marginally greater than the sum of the van der Waals radii, entirely consistent with the notion that this criterion is not absolute [91–93].

In terms of chemistry, 59 of the 62 examples are organomercury thiolates with only three examples of diorganomercury species covered in this survey. This observation clearly relates to the reduced Lewis basicity of the mercury centre in diorganomercury compounds. Indeed, only three out of a possible 46 diorganomercury compounds also possessing sulphur in the crystal included in the CSD [34] form Hg...S interactions in their crystals. The situation is rather different for organomercury thiolates where 60 out of possible 118 candidates form Hg...S interactions in their crystals.

## 5. Conclusions

The present survey has demonstrated the importance of Hg...S interactions in assembling molecules into zero-, one- and, less frequently, two-dimensional aggregation patterns. For the zero-dimensional aggregates, eight-membered  $\{\cdots\text{HgSCS}\}_2$  and four-membered  $\{\cdots\text{HgS}\}_2$  synthons dominate. A wide variety of topologies are apparent for the one-dimensional aggregation patterns. While a few exceptions exist, the mercury atom usually engages in only a single Hg...S contact. In terms of the propensity of formation, for an organomercury thiolate, it is nearly 50% likely that an intermolecular Hg...S interaction will form, an observation related to the thiophilic nature of mercury but also to the ready accessibility to mercury, being normally found within a linear C–Hg–S coordination environment, sometimes accompanied by weaker intramolecular Hg...S, Hg...S or Hg...S contacts. Clearly, there is enormous scope to further develop the supramolecular chemistry of organomercury thiolates, at least from a crystal engineering perspective.

**Supplementary Materials:** The following supporting information can be downloaded at: <https://www.mdpi.com/article/10.3390/cryst13030385/s1>, Figure S1. IHOLEW (2-Aminocyclopent-1-ene-1-carbodithioato)-methyl-mercury(II); Figure S2. CEJNUB tris( $\mu$ 2-Perfluoro-*o*-phenylene)-tri-mercury bis(dimethyl(4-nitrophenyl)-thiophosphate); Figure S3. FUPFEC ((N-Isopropyl-N-(ferrocenyl)methyl)dithiocarbamato)-phenyl-mercury; Figure S4. FOKBIQ Phenyl-(diethylthiocarbamato)-mercury(II); Figure S5. LUWZOU (4-Hydroxypiperidine-1-carbodithioato)-phenyl-mercury(II) chloroform solvate; Figure S6. MEDTHG Methyl-(N,N-diethylthiocarbamato)-mercury(II); Figure S7. FUPFIG ((N-butyl-N-(ferrocenyl)methyl)dithiocarbamato)-phenyl-mercury(II); Figure S8. YOLJAL (Morpholinedithiocarbamato)-phenyl-mercury(II); Figure S9. EKUYUT Phenyl-((furan-2-ylmethyl(ferrocenylmethyl)amino)dithiocarbamato)-mercury(II); Figure S10. GUVQUJ Phenyl-(N,N-di-n-propyldithiocarbamato-S,S')-mercury(II); Figure S11. EKUYON Phenyl-((ferrocenylmethyl(4-pyridinylmethyl)amino)dithiocarbamato)-mercury(II); Figure S12. FODRUN (N-(4-Pyridylmethyl)-N-(pyrrol-2-yl)dithiocarbamato-S,S')-phenyl-mercury(II) methanol solvate; Figure S13. YOLHUD (Di-n-butylthiocarbamato)-phenyl-mercury(II); Figure S14. FUPFAY ((N-benzyl-N-(ferrocenyl)methyl)dithiocarbamato)-phenyl-mercury(II); Figure S15. NEGRID (N-furfuryl-N-(2-phenylethyl)dithiocarbamato-S,S')-phenyl-mercury(II); Figure S16. HEGGOS (dimethylcarbamodithioato)-phenyl-mercury(II); Figure S17. YOMXUV Phenyl-(thiomorpholine-4-carbodithioato)-mercury(II); Figure S18. LAJGOV (4-(Dimethylamino)phenyl)-(O-methyl carbonodithioato)-mercury; Figure S19. YAHFIW (Diethylthiophosphate)-phenyl-mercury(II); Figure S20. VIHCUK Methyl-(diphenyldithiophosphinate)-mercury(II); Figure S21. BEBLUP 2-Dimethylaminothiophenolato-phenyl-mercury(II); Figure S22. VIYLAR Ethyl-((hydroxy-O)(diphenyl)(2-(sulfanyl-S)-3-(trimethylsilyl)phenyl)-phosphoniumato)-mercury methanol solvate; Figure S23. BORCIV (N-(1-(2-Hydroxyphenyl)ethylidene)-4-morpholinecarbohydrazonothioato-S)-(phenyl)-mercury; Figure S24. VIYLIZ ( $\mu$ 2-bis(3-Trimethylsilylphenyl-2-thiolato)phenyl(oxo)phosphanyl-S,S)-diethyl-di-mercury(II); Figure S25. NEFDEH Methyl-(2-nitrobenzenethiolato)-mercury(II); Figure S26. JETYEM Methyl-(2,4,6-tri-isopropylbenzenethiolato)-mercury(II); Figure S27. PAVVOY

(Cyclohexanone thiosemicarbazonato-N,S)-phenyl-mercury(II); Figure S28. DOMCAJ01 Methyl-(pyridine-2-thiolato-S)-mercury(II); Figure S29. HUBRON bis( $\mu$ -2,4,5-Disulfanyl-1,3-dithiol-2-one)-tetraphenyl-tetra-mercury; Figure S30. CIJPOB (Hydrogen tris(2-mercapto-1-t-butylimidazolyl)borate-S)-methyl-mercury(II) acetonitrile tetra-solvate; Figure S31. CIJPIV (Hydrogen tris(2-mercapto-1-t-butylimidazolyl)borate-S)-methyl-mercury(II); Figure S32. CIJQAO (Hydrogen tris(2-mercapto-1-t-butylimidazolyl)borate-S)-ethyl-mercury(ii) acetone hemi-solvate; Figure S33. KAPWUT ( $\mu$ -1,3,4-Thiadiazole-2,5-dithiolato-S,S')-bis(methyl-mercury(II)); Figure S34. FAZBOX ( $\mu$ -o-Phenylene)-bis(O-methyl-xanthato-S)-di-mercury dichloromethane mono-solvate; Figure S35. QUGVUJ (4-(o-Hydroxybenzylideneamino)phenylthiolato)-methyl-mercury(II); Figure S36. XUYROY 4-(Tri-t-butoxysilylthiomercurio)benzoic acid; Figure S37. FOKBEM Phenyl-(isopropylxanthate-S)mercury(II); Figure S38. LENZIN (Diethyldithiophosphinato-S)-phenyl-mercury(II); Figure S39. QIQHIH (2-Pyridylthiolato)-trichlorovinyl-mercury(II); Figure S40. XUHREY Ethyl-(2-carboxybenzenethiolato)-mercury(II); Figure S41. WAYPAN Trimethyl-( $\mu$ -3,1,1,1-tris(mercaptomethyl)ethane-S,S',S'')-tri-mercury(II); Figure S42. OBIZAC (1,5-bis(2-Methoxyphenyl)thiocarbazonato)-phenyl-mercury(II); Figure S43. NESRUA (N'-Benzylidene-N,N-dimethylcarbamohydrazonothioato)-(methyl)mercury(II); Figure S44. DOYFIG Methyl-(2-mercapto-4-methylpyrimidinato)-mercury(II); Figure S45. QUGVIX (3-Aminophenylthiolato)-phenyl-mercury(II); Figure S46. DOFNOC Ethyl-(phenylthiolato)-mercury(II); Figure S47. YOMXIJ (( $\mu$ -2-(furylmethyl)(4-(((2-furylmethyl)(sulfanyl)(thioxo)methyl)amino)methyl)-benzyl)carbamodithioato)-diphenyl-di-mercury; Figure S48. XUHREY01 Ethyl-(2-carboxybenzenethiolato)-mercury(II); Figure S49. PHGMSP Phenylmercury-(2,6-dimethyl-thiophenolate); Figure S50. OCOLEY (4,5-Diphenyl-(1,2,4)triazine-3-thionato)-methyl-mercury; Figure S51. LAWTUB Phenyl(phenylmethanethiolato)mercury(II); Figure S52. GILNOE bis(Methylene(diphenyl)thiophosphinate)-mercury(II); Figure S53. CHMEHG ( $\mu$ -trans-Cyclohexane-1,2-dithiolato)-bis(methyl-mercury(II)) 1980; Figure S54. LOPGUT ( $\mu$ -2,4-Pyrimidinedithiolato)-diphenyl-di-mercury(II); Figure S55. FUPFOM ( $\mu$ -2-N,N'-(1,3-dimethylphenylene)-bis(ferrocenylmethyl)dithiocarbamato))-bis(phenyl-mercury) diethyl ether solvate; Figure S56. CECWOW 8-Mercaptoquinolinato-phenyl-mercury(II); Figure S57. IHOLEW01 (2-Aminocyclopent-1-ene-1-carbodithioato)-methyl-mercury(II); Figure S58. QUGVOD (3-(o-Hydroxybenzylideneamino)phenylthiolato)-methyl-mercury(II); Figure S59. DOFNIW Methyl-(phenylthiolato)-mercury(II); Figure S60. IHOLIA (2-Aminocyclopent-1-ene-1-carbodithioato)-phenyl-mercury(II); Figure S61. EBUSIF Phenyl-(benzyl(pyridin-4-ylmethyl)carbamodithioato)-mercury(II); Figure S62. COCJUC catena-(bis( $\mu$ -Pyridin-4-yl)-bis(O,O'-di-isopropyl)dithiophosphato)-mercury-nickel(II).

**Funding:** This research was funded by the Sunway University Sdn Bhd, grant number GRTIN-RRO-56-2022.

**Institutional Review Board Statement:** Not applicable.

**Informed Consent Statement:** Not applicable.

**Data Availability Statement:** Not applicable.

**Conflicts of Interest:** The author declares no conflict of interest.

## References

1. Alcock, N.W. Secondary bonding to nonmetallic elements. *Adv. Inorg. Chem. Radiochem.* **1972**, *15*, 1–58. [[CrossRef](#)]
2. Mulliken, R.S. Structures of complexes formed by halogen molecules with aromatic and with oxygenated solvents. *J. Am. Chem. Soc.* **1950**, *72*, 600–608. [[CrossRef](#)]
3. Bent, H.A. Structural chemistry of donor-acceptor interactions. *Chem. Rev.* **1968**, *68*, 587–648. [[CrossRef](#)]
4. Hassel, O. Structural Aspects of interatomic charge-transfer bonding. *Science* **1970**, *170*, 497–502. [[CrossRef](#)]
5. Bauzá, A.; Alkorta, I.; Elguero, J.; Mooibroek, T.J.; Frontera, A. Spodium bonds: Noncovalent interactions involving Group 12 elements. *Angew. Chem. Int. Ed.* **2020**, *59*, 17482–17487. [[CrossRef](#)]
6. Alkorta, I.; Elguero, J.; Frontera, A. Not only hydrogen bonds: Other noncovalent interactions. *Crystals* **2020**, *10*, 180. [[CrossRef](#)]
7. Grabowski, S.J. The nature of triel bonds, a case of B and Al centres bonded with electron rich sites. *Molecules* **2020**, *25*, 2703. [[CrossRef](#)] [[PubMed](#)]
8. Jabłoński, M. Study of beryllium, magnesium, and spodium bonds to carbenes and carbodiphosphoranes. *Molecules* **2021**, *26*, 2275. [[CrossRef](#)]
9. Tiekink, E.R.T.; Winter, G. Inorganic xanthates: A structural perspective. *Rev. Inorg. Chem.* **1992**, *12*, 183–302. [[CrossRef](#)]

10. Haiduc, I.; Sowerby, D.B. Stereochemical aspects of phosphor-1,1-dithiolato metal complexes: Coordination patterns, molecular structures and supramolecular associations in dithiophosphinates and related compounds. *Polyhedron* **1996**, *15*, 2469–2521. [[CrossRef](#)]
11. Cox, M.J.; Tiekink, E.R.T. The diverse coordination patterns in the structures of zinc, cadmium and mercury bis(1,1-dithiolates). *Rev. Inorg. Chem.* **1997**, *17*, 1–23. [[CrossRef](#)]
12. Tiekink, E.R.T. Molecular architecture and supramolecular association in the zinc-triad 1,1-dithiolates. Steric control as a design element in crystal engineering? *CrystEngComm* **2003**, *5*, 101–113. [[CrossRef](#)]
13. Tiekink, E.R.T.; Haiduc, I. Stereochemical aspects of metal xanthate complexes: Molecular structures and supramolecular self-assembly. *Prog. Inorg. Chem.* **2005**, *54*, 127–319. [[CrossRef](#)]
14. Tiekink, E.R.T. Exploring the topological landscape exhibited by binary zinc-triad 1,1-dithiolates. *Crystals* **2018**, *8*, 292. [[CrossRef](#)]
15. Mahmoudi, G.; Masoudiasl, A.; Babashkina, M.G.; Frontera, A.; Doert, T.; White, J.M.; Zangrando, E.; Fedor, I.; Zubkov, F.I.; Safin, D.A. On the importance of  $\pi$ -hole spodium bonding in tricoordinated Hg<sup>II</sup> complexes. *Dalton Trans.* **2020**, *49*, 17547–17551. [[CrossRef](#)]
16. Mahmoudi, G.; Lawrence, S.E.; Cisterna, J.; Cárdenas, A.; Brito, I.; Frontera, A.; Safin, D.A. A new spodium bond driven coordination polymer constructed from mercury(II) azide and 1,2-bis(pyridin-2-ylmethylene)hydrazine. *New J. Chem.* **2020**, *44*, 21100–21107. [[CrossRef](#)]
17. Gomila, R.M.; Bauzá, A.; Mooibroek, T.J.; Frontera, A. Spodium bonding in five coordinated Zn(II): A new player in crystal engineering? *CrystEngComm* **2021**, *23*, 3084–3093. [[CrossRef](#)]
18. Gomila, R.M.; Bauzá, A.; Mooibroek, T.J.; Frontera, A.  $\pi$ -Hole spodium bonding in tri-coordinated Hg(II) complexes. *Dalton Trans.* **2021**, *50*, 7545–7553. [[CrossRef](#)]
19. Alizadeh, V.; Mahmoudi, G.; Vinokurova, M.A.; Pokazeev, K.M.; Alekseeva, K.A.; Miroslaw, B.; Khandar, A.A.; Frontera, A.; Safin, D.A. Spodium bonds and metal–halogen  $\cdots$ halogen–metal interactions in propagation of monomeric units to dimeric or polymeric architectures. *J. Mol. Struct.* **2022**, *1252*, 132144. [[CrossRef](#)]
20. Ciancaleoni, G.; Rocchigiani, L. Assessing the orbital contribution in the “spodium bond” by natural orbital for chemical valence–charge displacement analysis. *Inorg. Chem.* **2021**, *60*, 4683–4692. [[CrossRef](#)]
21. Basak, T.; Gomila, R.M.; Frontera, A.; Chattopadhyay, S. Differentiating intramolecular spodium bonds from coordination bonds in two polynuclear zinc(II) Schiff base complexes. *CrystEngComm* **2021**, *23*, 2703–2710. [[CrossRef](#)]
22. Kumar, P.; Frontera, A.; Pandey, S.K. Coordination versus spodium bonds in dinuclear Zn(II) and Cd(II) complexes with a dithiophosphate ligand. *New J. Chem.* **2021**, *45*, 19402–19415. [[CrossRef](#)]
23. Kumar, P.; Banerjee, S.; Radha, A.; Firdoos, T.; Sahoo, S.C.; Pandey, S.K. Role of non-covalent interactions in the supramolecular architectures of mercury(II) diphenyldithiophosphates: An experimental and theoretical investigation. *New J. Chem.* **2021**, *45*, 2249–2263. [[CrossRef](#)]
24. Wysokiński, R.; Zierkiewicz, W.; Michalczyk, M.; Scheiner, S. Anion  $\cdots$ anion (MX<sub>3</sub><sup>−</sup>)<sub>2</sub> dimers (M = Zn, Cd, Hg; X = Cl, Br, I) in different environments. *Phys. Chem. Chem. Phys.* **2021**, *23*, 13853–13861. [[CrossRef](#)]
25. Llull, R.; Montalbán, G.; Vidal, I.; Gomila, R.M.; Bauzá, A.; Frontera, A. Theoretical study of spodium bonding in the active site of three Zn-proteins and several model systems. *Phys. Chem. Chem. Phys.* **2021**, *23*, 16888–16896. [[CrossRef](#)]
26. Rozhkov, A.V.; Katlenok, E.A.; Zhmykhova, M.V.; Kuznetsov, M.L.; Khrustalev, V.N.; Tugashov, K.I.; Bokach, N.A.; Kukushkin, V.Y. Spodium bonding to anticrown-Hg<sub>3</sub> boosts phosphorescence of cyclometalated-Pt<sup>II</sup> complexes. *Inorg. Chem. Front.* **2023**, *10*, 493–510. [[CrossRef](#)]
27. Tiekink, E.R.T.; Zukerman-Schpector, J. Stereochemical activity of lone pairs of electrons and supramolecular aggregation patterns based on secondary interactions involving tellurium in its 1,1-dithiolate structures. *Coord. Chem. Rev.* **2010**, *254*, 46–76. [[CrossRef](#)]
28. Lee, S.M.; Heard, P.J.; Tiekink, E.R.T. Molecular and supramolecular chemistry of mono- and di-selenium analogues of metal dithiocarbamates. *Coord. Chem. Rev.* **2018**, *375*, 410–423. [[CrossRef](#)]
29. Tiekink, E.R.T. A survey of supramolecular aggregation based on main group element  $\cdots$ selenium secondary bonding interactions—A survey of the crystallographic literature. *Crystals* **2020**, *10*, 503. [[CrossRef](#)]
30. Tiekink, E.R.T. Zero-, one-, two- and three-dimensional supramolecular architectures sustained by Se  $\cdots$ O chalcogen bonding: A crystallographic survey. *Coord. Chem. Rev.* **2021**, *427*, 213586. [[CrossRef](#)]
31. Tiekink, E.R.T. Supramolecular aggregation patterns featuring Se  $\cdots$ N secondary-bonding interactions in mono-nuclear selenium compounds: A comparison with their congeners. *Coord. Chem. Rev.* **2021**, *443*, 214031. [[CrossRef](#)]
32. Tiekink, E.R.T. Te  $\cdots$ N secondary-bonding interactions in tellurium crystals: Supramolecular aggregation patterns and a comparison with their lighter congeners. *Coord. Chem. Rev.* **2022**, *457*, 214397. [[CrossRef](#)]
33. Tiekink, E.R.T. Supramolecular architectures featuring Se  $\cdots$ N secondary-bonding interactions in crystals of selenium-rich molecules: A comparison with their congeners. *CrystEngComm* **2023**, *25*, 9–39. [[CrossRef](#)]
34. Groom, C.R.; Bruno, I.J.; Lightfoot, M.P.; Ward, S.C. The Cambridge Structural Database. *Acta Crystallogr. B Struct. Sci. Cryst. Eng. Mater.* **2016**, *72*, 171–179. [[CrossRef](#)] [[PubMed](#)]
35. Spek, A.L. checkCIF validation ALERTS: What they mean and how to respond. *Acta Crystallogr. Sect. E Crystallogr. Commun.* **2020**, *76*, 1–11. [[CrossRef](#)]
36. Brandenburg, K.; Berndt, M. *DIAMOND, Version 3.2k*; GbR: Bonn, Germany, 2006.

37. Bruno, I.J.; Cole, J.C.; Edgington, P.R.; Kessler, M.; Macrae, C.F.; McCabe, P.; Pearson, J.; Taylor, R. New software for searching the Cambridge Structural Database and visualizing crystal structures. *Acta Crystallogr. Sect. B Struct. Sci. Cryst. Eng. Mater.* **2002**, *58*, 389–397. [[CrossRef](#)]
38. Tsunoda, M.; Gabbai, F.P. Complexation of methylparathion and bis(2-hydroxyethyl)sulfide by the tridentate lewis acid [(o-C<sub>6</sub>F<sub>4</sub>Hg)<sub>3</sub>]. *Heteroat. Chem.* **2005**, *16*, 292–297. [[CrossRef](#)]
39. Lai, C.S.; Tiekink, E.R.T. Supramolecular association in organomercury(II) 1,1-dithiolates. Complementarity between Hg···S and hydrogen bonding interactions in organomercury(II) 2-amino-cyclopent-1-ene-1-carbodithioates. *CrystEngComm* **2003**, *5*, 253–261. [[CrossRef](#)]
40. Singh, N.; Kumar, A.; Prasad, R.; Molloy, K.C.; Mahon, M.F. Syntheses, crystal, photoluminescence and electrochemical investigation of some new phenylmercury(II) dithiocarbamate complexes involving ferrocene. *Dalton Trans.* **2010**, *39*, 2667–2675. [[CrossRef](#)]
41. Tiekink, E.R.T. Phenylmercury dithiolates. The crystal and molecular structures of (C<sub>6</sub>H<sub>5</sub>Hg(S<sub>2</sub>COR) (R = Me; iPr and (C<sub>6</sub>H<sub>5</sub>)Hg(S<sub>2</sub>CNEt<sub>2</sub>)). *J. Organomet. Chem.* **1987**, *322*, 1–10. [[CrossRef](#)]
42. Prasad, R.; Yadav, R.; Trivedi, M.; Kociok-Köhn, G.; Kumar, A. The interplay of thiophilic and hydrogen bonding interactions in the supramolecular architecture of phenylmercury 4-hydroxypiperidine dithiocarbamate. *J. Mol. Struct.* **2016**, *1103*, 265–270. [[CrossRef](#)]
43. Chieh, C.; Leung, L.P.C. Crystal structure and vibrational spectra of methyl N,N-diethyldithiocarbamate mercury(II). *Can. J. Chem.* **1976**, *54*, 3077–3084. [[CrossRef](#)]
44. Singh, N.; Kumar, A.; Molloy, K.C.; Mahon, M.F. Syntheses, crystal and molecular structures, and properties of some new phenylmercury(II) dithiolate complexes. *Dalton Trans.* **2008**, 4999–5007. [[CrossRef](#)] [[PubMed](#)]
45. Singh, V.; Chauhan, R.; Kumar, A.; Bahadur, L.; Singh, N. Efficient phenylmercury(II) methylferrocenyldithiocarbamate functionalized dye-sensitized solar cells. *Dalton Trans.* **2010**, *39*, 9779–9788. [[CrossRef](#)] [[PubMed](#)]
46. Lai, C.S.; Tiekink, E.R.T. Phenyl(N,N-di-n-propyldithiocarbamate)mercury(II). *Appl. Organomet. Chem.* **2003**, *17*, 194. [[CrossRef](#)]
47. Singh, V.; Kumar, V.; Gupta, A.N.; Drew, M.G.B.; Singh, N. Effect of pyridyl substituents leading to the formation of green luminescent mercury(II) coordination polymers, zinc(II) dimers and a monomer. *New J. Chem.* **2014**, *38*, 3737–3748. [[CrossRef](#)]
48. Selvaganapathi, P.; Thirumaran, S.; Ciattini, S. Synthesis, spectral, crystal structures, Hirshfeld surface analysis and DFT studies on phenylmercury(II) dithiocarbamate complexes and their utility for the preparation of mercury sulfide nanoparticles. *J. Mol. Struct.* **2017**, *1148*, 547–556. [[CrossRef](#)]
49. Cadar, O.; Pöllnitz, A.; Mărgineanu, D.; Silvestru, C. Solid-state structure and solution behaviour of organomercury(II) compounds containing 2-(Me<sub>2</sub>NCH<sub>2</sub>)C<sub>6</sub>H<sub>4</sub>- moieties. Supramolecular aspects. *Inorg. Chim. Acta* **2017**, *479*, 90–97. [[CrossRef](#)]
50. Yadav, M.K.; Rajput, G.; Gupta, A.N.; Kumar, V.; Drew, M.G.B.; Singh, N. Exploring the coordinative behaviour and molecular architecture of new PhHg(II)/Hg(II) dithiocarbamate complexes. *Inorg. Chim. Acta* **2014**, *421*, 210–217. [[CrossRef](#)]
51. Abu-salem, Q. Synthesis, structural characterization and supramolecularity of (O-methyl dithiocarbonato)(N,N-dimethylaminophenyl) mercury(II). *Synth. React. Inorg. Met.-Org. Nano-Met. Chem.* **2016**, *46*, 821–827. [[CrossRef](#)]
52. Vázquez-López, E.M.; Castiñeiras, A.; Sánchez, A.; Casas, J.S.; Sordo, J. Phenylmercury(II) dithiophosphates. Crystal structure of (O,O'-diethyldithiophosphate) phenylmercury(II). *J. Crystallogr. Spectrosc. Res.* **1992**, *22*, 403–409. [[CrossRef](#)]
53. Zukerman-Schpector, J.; Vázquez-López, E.M.; Sánchez, A.; Casas, J.S.; Sordo, J. Synthesis and structural characterization of diphenyldithiophosphinates of methyl- and phenylmercury(II). Crystal structure of MeHgS<sub>2</sub>PPh<sub>2</sub>. *J. Organomet. Chem.* **1991**, *405*, 67–74. [[CrossRef](#)]
54. Tiekink, E.R.T. Aggregation patterns in the crystal structures of organometallic Group XV 1,1-dithiolates: The influence of the Lewis acidity of the central atom, metal- and ligand- bound steric bulk, and coordination potential of the 1,1-dithiolate ligands upon supramolecular architecture. *CrystEngComm* **2006**, *8*, 104–118. [[CrossRef](#)]
55. Kuz'mina, L.G.; Struchkov, Y.T.; Rokhlina, E.M.; Peregudov, A.S.; Kravtsov, D.N. An X-ray structural study of non-valence interactions and coordination in organometallic compounds. 20. The crystal-structure of phenylmercury 2-dimethylaminothiophenolate. *J. Struct. Chem.* **1981**, *22*, 718–723. [[CrossRef](#)]
56. Fernández, P.; Sousa-Pedrares, A.; Romero, J.; García-Vázquez, J.A.; Sousa, A.; Pérez-Lourido, P. Zinc(II), cadmium(II), mercury(II), and ethylmercury(II) complexes of phosphinothiol ligands. *Inorg. Chem.* **2008**, *47*, 2121–2132. [[CrossRef](#)] [[PubMed](#)]
57. Biswas, S.; Mostafa, G.; Steele, I.M.; Sarkar, S.; Dey, K. Synthesis, crystal structures and luminescent properties of phenylmercury(II) complexes with thiohydrazone ligands having weak Hg···π and Hg···Hg interactions. *Polyhedron* **2009**, *28*, 1010–1016. [[CrossRef](#)]
58. Aupers, J.H.; Howie, R.A.; Wardell, J.L. Structure of methyl(o-nitrobenzenethiolato)mercury. *Polyhedron* **1997**, *16*, 2283–2289. [[CrossRef](#)]
59. Block, E.; Brito, M.; Gernon, M.; McGowty, D.; Kang, H.; Zubieta, J. Mercury(II) and methylmercury(II) complexes of novel sterically hindered thiolates: Carbon-13 and mercury-199 NMR studies and the crystal and molecular structures of [MeHg(SC<sub>6</sub>H<sub>2</sub>-2,4,6-Pr-is<sub>3</sub>)], [Hg(SC<sub>6</sub>H<sub>4</sub>-2-SiMe<sub>3</sub>)<sub>2</sub>], [Hg(2-SC<sub>5</sub>H<sub>3</sub>N-3-SiMe<sub>3</sub>)<sub>2</sub>], and [Hg{(2-SC<sub>6</sub>H<sub>4</sub>)<sub>2</sub>SiMe<sub>2</sub>}]<sub>2</sub>. *Inorg. Chem.* **1990**, *29*, 3172–3181. [[CrossRef](#)]
60. Lobana, T.S.; Rekha; Butcher, R.J.; Failes, T.W.; Turner, P. Crystal structures of organomercury(II) derivatives of cyclohexanone and benzaldehyde thiosemicarbazones. *J. Coord. Chem.* **2005**, *58*, 1369–1375. [[CrossRef](#)]

61. Castiñeiras, A.; Hiller, W.; Strähle, J.; Bravo, J.; Casas, J.S.; Gayoso, M.; Sordo, J. Methyl- and phenyl-mercury(II) derivatives of 2-mercaptopyridine. Crystal and molecular structure of methyl(pyridine-2-thiolato)mercury(II). *J. Chem. Soc. Dalton Trans.* **1948**, 1945–1948. [[CrossRef](#)]
62. Martins, C.X.; Ferreira, G.B.; Howie, R.A.; Bordinhão, J.; Comerlato, N.M.; Wardell, J.L.; Wardell, S.M.S.V. Syntheses of bis(organomercury)1,3-dithiole-2-thione-4,5-dithiolates and related compounds: Crystal structure of bis(phenylmercury)1,3-dithiole-2-one-4,5-dithiolate. *Inorg. Chim. Acta* **2015**, *429*, 189–194. [[CrossRef](#)]
63. Melnick, J.G.; Parkin, G. Cleaving mercury-alkyl bonds: A functional model for mercury detoxification by MerB. *Science* **2007**, *317*, 225–227. [[CrossRef](#)] [[PubMed](#)]
64. Castaño, M.V.; Plasencia, M.M.; Macias, A.; Casas, J.S.; Sordo, J.; Castellano, E.E. Preparation and crystal structure of a binuclear compound of methylmercury(II) containing bismuthiol I as a bridging ligand. *Dalton Trans.* **1989**, 1409–1411. [[CrossRef](#)]
65. Tiekink, E.R.T. Crystal structure of a 1,2-phenylenedimercury dixanthate. *J. Organomet. Chem.* **1986**, *303*, C53–C55. [[CrossRef](#)]
66. Almagro, X.; Clegg, W.; Cucurull-Sánchez, L.; González-Duarte, P.; Traveria, M. Schiff bases derived from mercury(II)-aminothiolate complexes as metalloligands for transition metals. *J. Organomet. Chem.* **2001**, *623*, 137–148. [[CrossRef](#)]
67. Chojnacki, J.; Walaszewska, A.; Baum, E.; Wojnowski, W. 4-(Tri-tert-butoxysilylthiomercuro)benzoic acid. *Acta Crystallogr. Sect. E Struct. Rep.* **2003**, *59*, m125–m127. [[CrossRef](#)]
68. Lafrance-Vanasse, J.; Maryse Lefebvre, M.; Di Lello, P.; Sygusch, J.; Omichinski, J.G. Crystal structures of the organomercurial lyase MerB in its free and mercury-bound forms: Insights into the mechanism of methylmercury degradation. *J. Biol. Chem.* **2009**, *284*, 938–944. [[CrossRef](#)]
69. Casas, J.S.; Castiñeiras, A.; Sánchez, A.; Sordo, J.; Vázquez-López, E.M. Dicyclohexyldithiophosphinates and diethyldithiophosphinates of methylmercury(II) and phenylmercury(II): Crystal and molecular structure of [HgPh(S<sub>2</sub>PEt<sub>2</sub>)]. *J. Organomet. Chem.* **1984**, *468*, 1–6. [[CrossRef](#)]
70. Bell, N.A.; Gelbrich, T.; Hursthouse, M.B.; Light, M.E.; Wilson, A. Reactions of trichlorovinylmercurials with potential non-chelating bidentate ligands. Crystal structures of [(C<sub>2</sub>Cl<sub>3</sub>)<sub>2</sub>Hg(4,4'-bipyridyl)] (1), [C<sub>2</sub>Cl<sub>3</sub>Hg(2-pyridyl thiolate)] (12) and polymeric HgBr<sub>2</sub>(2,2'-dipyridyl disulfide) (10). *Polyhedron* **2000**, *19*, 2539–2546. [[CrossRef](#)]
71. Sattler, W.; Yurkerwich, K.; Parkin, G. Molecular structures of protonated and mercurated derivatives of thimerosal. *Dalton Trans.* **2009**, 4327–4333. [[CrossRef](#)]
72. Ghilardi, C.A.; Midollini, S.; Orlandini, A.; Vacca, A. Reactivity of the tripodal trithiol 1,1,1-tris(mercaptomethyl)ethane toward methyl- and ethyl-mercury halides. *J. Chem. Soc. Dalton Trans.* **1993**, 3117–3121. [[CrossRef](#)]
73. von Eschwege, K.; Muller, F.; Muller, A. [1,5-Bis(2-methoxyphenyl)thiocarbazonato-κ<sup>2</sup>N<sup>1</sup>,S]phenylmercury(II). *Acta Crystallogr. Sect. E Struct. Rep.* **2011**, *67*, m1804. [[CrossRef](#)] [[PubMed](#)]
74. López-Torres, E.; Mendiola, M.A. Synthesis and molecular structures of methyl and phenylmercury(II) complexes with benzaldehyde-4,4-dimethylthiosemicarbazone. *J. Organomet. Chem.* **2013**, *725*, 28–33. [[CrossRef](#)]
75. Bravo, J.; Casas, J.S.; Mascarenhas, Y.P.; Sánchez, A.; Santos, C.; Deo, P.; Sordo, J. Methyl(2-mercapto-4-methylpyrimidinato)mercury(II): A methylmercury(II) derivative with an unusual metal–metal interaction. *J. Chem. Soc. Chem. Comm.* **1986**, 1100–1101. [[CrossRef](#)]
76. Melnick, J.G.; Yurkerwich, K.; Buccella, D.; Sattler, W.; Parkin, G. Molecular structures of thimerosal (Merthiolate) and other arylthiolate mercury alkyl compounds. *Inorg. Chem.* **2008**, *47*, 6421–6426. [[CrossRef](#)] [[PubMed](#)]
77. Kuz'mina, L.G.; Bokii, N.G.; Struchkov, Y.T.; Kravtsov, D.N.; Rokhlina, E.M. X-ray diffraction investigation of nonvalent interactions and coordination in organometallic compounds IV. Crystal and molecular structure of phenylmercury 2,6-dimethylthiophenolate. *J. Struct. Chem.* **1974**, *15*, 419–423. [[CrossRef](#)]
78. López-Torres, E.; Mendiola, M.A.; Pastor, C.J. Mercury and methylmercury complexes with a triazine-3-thione ligand. *Polyhedron* **2006**, *25*, 1464–1470. [[CrossRef](#)]
79. Nath, P.; Bharty, M.K.; Gupta, S.K.; Butcher, R.J.; Jasinski, J.P. (Benzylthiolato-κS)phenylmercury(II). *IUCrData* **2017**, *2*, x170503. [[CrossRef](#)]
80. Wang, S.; Fackler, J.P., Jr. Organobimetallic complexes with Hg[CH<sub>2</sub>P(S)Ph<sub>2</sub>]<sub>2</sub>. Syntheses and characterization of two structural isomers of [HgAu(CH<sub>2</sub>P(S)Ph<sub>2</sub>)<sub>2</sub>]PF<sub>6</sub> and the mercury precursor. *Organometallics* **1988**, *7*, 2415–2417. [[CrossRef](#)]
81. Alcock, N.W.; Lampe, P.A.; Moore, P. Complexes of methylmercury(II) with dithiol ligands: Spectroscopic and crystallographic studies. The crystal structure of trans-1,2-dimercaptocyclohexanebis[methylmercury(II)], [Hg<sub>2</sub>Me<sub>2</sub>(S<sub>2</sub>C<sub>6</sub>H<sub>10</sub>)]. *J. Chem. Soc. Dalton Trans.* **1980**, 1471–1474. [[CrossRef](#)]
82. Lemos, S.S.; Martins, D.U.; Deflon, V.M.; Elena, J. Cationic and neutral phenylmercury(II) complexes with heterocyclic thione ligands. X-ray structures of [HgPh(dmpymtH)][BF<sub>4</sub>]·H<sub>2</sub>O and [{HgPh}<sub>2</sub>(μ-dtu)]. *Organometallics* **2009**, *694*, 253–258. [[CrossRef](#)]
83. Kuz'mina, L.G.; Struchkov, Y.T.; Rokhlina, E.M.; Kravtsov, D.N. X-ray structural study of nonvalence interactions and coordination in organometallic compounds. XXIV. Crystal-structure of phenylmercury quinoline-8-thiolate. *J. Struct. Chem.* **1983**, *24*, 764–770. [[CrossRef](#)]
84. Baker, J.P. Mercury, Vaccines, and Autism. *Am. J. Public Health* **2008**, *98*, 244–253. [[CrossRef](#)] [[PubMed](#)]
85. Schmidbaur, H.; Schier, A. Mercurophilic Interactions. *Organometallics* **2015**, *34*, 2048–2066. [[CrossRef](#)]
86. Singh, V.; Kumar, A.; Prasad, R.; Rajput, G.; Drew, M.G.B.; Singh, N. The interplay of secondary Hg···S, Hg···N and Hg···π bonding interactions in supramolecular structures of phenylmercury(II) dithiocarbamates. *CrystEngComm* **2011**, *13*, 6817–6826. [[CrossRef](#)]

87. Mocanu, T.; Kiss, L.; Sava, A.; Shova, S.; Silvestru, C.; Andruh, M. Coordination polymers and supramolecular solid-state architectures constructed from an organometallic tecton, bis(4-pyridyl)mercury. *Polyhedron* **2019**, *166*, 7–16. [[CrossRef](#)]
88. Tiekink, E.R.T. On the coordination role of pyridyl-nitrogen in the structural chemistry of pyridyl-substituted dithiocarbamate ligands. *Crystals* **2021**, *11*, 286. [[CrossRef](#)]
89. Dunitz, J.D.; Taylor, R. Organic fluorine hardly ever accepts hydrogen bonds. *Chem. Eur. J.* **1997**, *3*, 89–98. [[CrossRef](#)]
90. Tiekink, E.R.T.; Zukerman-Schpector, J. A structural survey of metal  $\cdot\cdot\cdot\pi$  heteroaromatic supramolecular synthons for metal = tellurium, tin, and gold. *CrystEngComm* **2009**, *11*, 2701–2711. [[CrossRef](#)]
91. Caracelli, I.; Haiduc, I.; Zukerman-Schpector, J.; Tiekink, E.R.T.  $M\cdot\cdot\cdot\pi$ (arene) interactions for M = gallium, indium and thallium: Influence upon supramolecular self-assembly and prevalence in some proteins. *Coord. Chem. Rev.* **2014**, *283*, 50–63. [[CrossRef](#)]
92. Balmohammadi, Y.; Khavasi, H.R.; Naghavi, S.S. Existence of untypical halogen-involving interactions in crystal packings: A statistical and first-principles study. *CrystEngComm* **2020**, *22*, 2756–2765. [[CrossRef](#)]
93. Politzer, P.; Murray, J.S. The use and misuse of van der Waals radii. *Struct. Chem.* **2021**, *32*, 623–629. [[CrossRef](#)]

**Disclaimer/Publisher's Note:** The statements, opinions and data contained in all publications are solely those of the individual author(s) and contributor(s) and not of MDPI and/or the editor(s). MDPI and/or the editor(s) disclaim responsibility for any injury to people or property resulting from any ideas, methods, instructions or products referred to in the content.